Maintenance of murine platelet homeostasis by the kinase Csk and phosphatase CD148

Mori, Jun; Nagy, Zoltan; Di Nunzio, Giada; Smith, Christopher W; Geer, Mitchell J; Al Ghaithi, Rashid; van Geffen, Johanna P; Heising, Silke; Boothman, Luke; Tullemans, Bibian M E; Correia, Joao; Tee, Louise; Kuijpers, Marijke J E; Harrison, Paul; Heemskerk, Johan W M; Jarvis, Gavin E; Tarakhovsky, Alexander; Weiss, Arthur; Mazharian, Alexandra; Senis, Yotis A

DOI:
10.1182/blood-2017-02-768077

Document Version
Peer reviewed version

Citation for published version (Harvard):
Mori, J, Nagy, Z, Di Nunzio, G, Smith, CW, Geer, MJ, Al Ghaithi, R, van Geffen, JP, Heising, S, Boothman, L, Tullemans, BME, Correia, J, Tee, L, Kuijpers, MJE, Harrison, P, Heemskerk, JWM, Jarvis, GE, Tarakhovsky, A, Weiss, A, Mazharian, A & Senis, YA 2018, 'Maintenance of murine platelet homeostasis by the kinase Csk and phosphatase CD148', *Blood*, vol. 131, no. 10. https://doi.org/10.1182/blood-2017-02-768077

Maintenance of murine platelet homeostasis by the kinase Csk and phosphatase CD148

Jun Mori,[1*] Zoltan Nagy,[1*] Giada Di Nunzio,[1] Christopher W. Smith,[1] Mitchell J. Geer,[1] Rashid Al Ghaithi,[2] Johanna P. van Geffen,[3] Silke Heising,[1] Luke Boothman,[1] Bibian M. E. Tullemans,[3] Joao N. Correia,[1] Louise Tee,[1] Marijke J. E. Kuijpers,[3] Paul Harrison,[2] Johan W. M. Heemskerk,[3] Gavin E. Jarvis,[4] Alexander Tarakhovsky,[5] Arthur Weiss,[6] Alexandra Mazharian[1] and Yotis A. Senis[1]

[1]Institute of Cardiovascular Sciences and [2]Institute of Inflammation and Ageing, College of Medical and Dental Sciences, University of Birmingham, Birmingham, UK; [3]Department of Biochemistry, Cardiovascular Research Institute Maastricht, Maastricht University, Maastricht, The Netherlands; [4]Department of Physiology, Development and Neuroscience, University of Cambridge, Cambridge, UK; [5]Laboratory of Immune Cell Epigenetics and Signaling, The Rockefeller University, New York, USA; [6]Department of Medicine, Rosalind Russell-Ephraim P. Engleman Rheumatology Research Center and Howard Hughes Medical Institute, University of California, San Francisco, USA

[*]JM and ZN contributed equally to this study

Correspondence: Yotis A. Senis, Institute of Cardiovascular Sciences, College of Medical and Dental Sciences, University of Birmingham, Birmingham, B15 2TT, UK; e-mail: y.senis@bham.ac.uk

Short title: Csk and CD148 regulate platelet homeostasis

Word count Abstract: 171 words

Word count of main text: 4,932

Total number of figures and tables: 1 Table and 7 Figures (1 Supplemental Table, 10 Supplemental Figures and 3 Videos)

Key Points

- Csk and CD148 are non-redundant regulators of SFKs in platelets and deletion of either induces cell-intrinsic negative feedback mechanisms
- Csk is a negative regulator of SFK activity, whereas CD148 is a dual positive and negative regulator of SFK activity in platelets

Abstract

Src family kinases (SFKs) coordinate the initiating and propagating activation signals in platelets, however it remains unclear how they are regulated. Here we show that ablation of C-terminal Src kinase (Csk) and receptor-like protein tyrosine-phosphatase CD148 in mice results in a dramatic increase in platelet SFK activity, demonstrating that these proteins are essential regulators of platelet reactivity. Paradoxically, Csk/CD148-deficient mice exhibit reduced *in vivo* and *ex vivo* thrombus formation and increased bleeding following injury, rather than a prothrombotic phenotype. This is a consequence of multiple negative feedback mechanisms, including downregulation of the immunoreceptor tyrosine-based activation motif (ITAM)- and hemi-ITAM-containing receptors GPVI-FcR γ-chain and CLEC-2, respectively and upregulation of the immunoreceptor tyrosine-based inhibition motif (ITIM)-containing receptor G6b-B and its interaction with the tyrosine phosphatases Shp1 and Shp2. Results from an analogue-sensitive Csk mouse model demonstrate the unconventional role of SFKs in activating ITIM signaling. This study establishes Csk and CD148 as critical molecular switches controlling the thrombotic and hemostatic capacity of platelets, and reveals cell-intrinsic mechanisms that prevent pathological thrombosis from occurring.

Introduction

Platelets are highly reactive fragments of megakaryocytes (MKs) that interrogate the vessel wall and prevent excessive blood loss following injury. They do so by adhering to exposed extracellular matrix proteins and forming a thrombus that transiently occludes the blood vessel, promoting wound repair and vessel regeneration. However, it remains unclear how the reactivity of platelets in the circulation is regulated.

Platelets contain high levels of Src family kinases (SFKs) that have a coordinating role in initiating and propagating primary activation signals.[1,2] The three most abundant SFKs in human and mouse platelets are Src, Lyn and Fyn (Figure S1).[3,4] Src and Fyn act primarily as positive regulators of platelet activation,[5-8] whereas Lyn is both a positive and negative regulator of activation.[9,10] SFKs are constitutively associated with the cytoplasmic tails of several important platelet receptors, including: the glycoprotein (GP)Ib-IX-V complex,[11,12] the immunoreceptor tyrosine-based activation motif (ITAM)-containing GPVI-FcR γ-chain receptor complex,[5,13] and the integrin αIIbβ3.[14,15] SFKs are also involved in transmitting secondary activation signals from G protein-coupled receptors.[16-21]

Equally important, but less well understood are the inhibitory functions of SFKs. Concomitant with phosphorylating ITAM-containing receptors activating platelets,[5,22] SFKs also phosphorylate immunoreceptor tyrosine-based inhibition motif (ITIM)-containing receptors that inhibit platelets.[23] The latter recruit SH2 domain-containing phosphatases, including the non-transmembrane protein-tyrosine phosphatases Shp1 and Shp2,[24-26] that inhibit platelet activation. The two most well characterized platelet ITIM-containing receptors are PECAM-1 and G6b-B, which inhibit platelet activation and modulate platelet homeostasis, respectively.[27,28]

Limited knowledge has been gained how platelet SFKs are regulated. SFKs are primed by dephosphorylation of the C-terminal inhibitory phospho-tyrosine residue by the

receptor-like tyrosine phosphatase CD45 in most hematopoietic cells,[29] and by CD148 in platelets.[30-32] Primed SFKs need to be fully activated through *trans*-auto-phosphorylation of a tyrosine residue located within the catalytic domain.[33] On the other hand, inactivation of SFKs can occur through the action of C-terminal Src kinase (Csk) and the structurally-related Csk homologous kinase (Chk), also referred to as megakaryocyte-associated tyrosine kinase (Matk), both of which target the C-terminal inhibitory tyrosine residue in SFKs.[34,35] However, it remains unknown how the threshold of individual SFK activation is set in platelets

To address these questions, we generated a series of MK-specific conditional *knockout (KO)* mouse models leading to deletion of *Csk*, *CD148* or *Csk/CD148*, and studied the consequences of these deletions for platelet physiology. Disruption of the homeostatic balance of SFK activity in MKs had dramatic and unexpected consequences on the number and reactivity of platelets in the circulation, due to cell-intrinsic negative feedback mechanisms, involving the ITIM-containing receptor G6b-B and Chk, culminating in anti-thrombotic and hemorrhagic outcomes.

Materials and methods

Mice

Csk$^{fl/fl}$, *CD148*$^{fl/fl}$, *Pf4-Cre*$^{+}$ and *Csk*^{AS} mice were generated, as previously described.[36-39] All mice were on a C57BL/6 background. All procedures were undertaken with United Kingdom Home Office approval in accordance with the Animals (Scientific Procedures) Act of 1986.

Antibodies and reagents

Thiazole orange (BD Retic-Count^{TM}) were from BD Bioscience. PP1 analogue IV (3-IB-PP1) was from Calbiochem. Antibodies are described in detail in Supplemental Methods.

Immune thrombocytopenia

Thrombocytopenia was induced as previously described.[28]

Platelet preparation

Blood was collected from terminally CO_2-narcosed mice from the abdominal vena cava into 1:10 (v:v) acid-citrate-dextrose anticoagulant. Washed platelets were prepared as previously described.[40] Adenosine diphosphate (ADP)-sensitive washed platelets were prepared in the presence of ADP scavenger apyrase as previously described.[41] Platelet counts were normalized and used for spreading (2×10^7/ml), aggregation (2×10^8/ml) or biochemical analysis ($4 - 5 \times 10^8$/ml).

Platelet functional assays and biochemistry

Platelet aggregation, adenosine triphosphate (ATP) secretion, spreading, clot retraction, platelet adhesion under flow, total thrombus-formation analysis system (T-TAS), stimulation

for biochemical analysis, immunoblotting and immunoprecipitation are described in detail in Supplemental Methods.

Flow cytometry

Reticulated platelets in blood were double stained with αIIb and thiazole orange (BD Retic-Count™, BD Bioscience). Surface protein expression was measured in blood or bone marrow cells with indicated FITC- or PE-conjugated antibodies by flow cytometry (BD Accuri C6 for platelets; BD FACSCalibur for bone marrow cells), as previously described.[25,28]

Tail bleeding assay

Experiments were performed on 8-10 week old *KO* and litter-matched *WT* mice as previously described.[30]

***In vivo* thrombosis assays**

Laser-induced injury of arterioles in the cremaster muscle and ferric chloride-induced injury of carotid arteries were performed and analyzed as previously described.[42]

Statistical analysis

Data presented are means ± standard errors of the mean (SEM). One-way or two-way ANOVA followed by *post-hoc* tests were used to determine statistical significance ($P < .05$). Further details on statistical analysis are provided in Supplemental Methods.

Results

Rescue of thrombocytopenia in Csk/CD148-deficient mice

MK-specific *Csk* and *CD148* conditional *KO* (*Csk* and *CD148 KO*) mice were generated by crossing $Csk^{fl/fl}$ and $CD148^{fl/fl}$ mice with *Pf4-Cre*$^{+}$ transgenic mice, respectively.[36-38] *Csk/CD148* conditional *double KO* (*DKO*) mice were also generated, to determine if deletion of both enzymes simultaneously would rescue phenotypes of single *KO* mice, and to reveal novel mechanisms of SFK regulation (Figure 1A).

Platelet count in *Csk KO* mice was reduced by 65% and platelet volume increased by 33% (Figure 1B and Table S1), suggesting defects in platelet production and/or clearance. This was supported by a 2-fold increase in the proportion of reticulated, immature platelets in these mice (Figures 1C and S2A). The same parameters were normal in *CD148 KO* mice (Figures 1B-C and S2A). While the platelet count was normal in *DKO* mice, the variability in numbers was greater than in *wild-type* (*WT*) and *Csk KO* mice, and the proportion of large, reticulated platelets was similar to that in *Csk KO* mice (Figures 1B-C, S2A and Table S1). Increased numbers of immune and granulocytic cells in *Csk* and *DKO* mice (Table S1) may be an indirect consequence of non-specific deletion of floxed *Csk* and *CD148* in other hematopoietic lineages by the *Pf4-Cre* transgene, which is reported to be *'leaky'*.[43] Interestingly, the proportion of P-selectin^{+}αIIb^{+} platelets were normal in *Csk KO* mice and only marginally elevated in *DKO* mice (Figure S2B), pointing to only minimal pre-activation of these platelets in the circulation or downregulation of activation markers.

To explore whether increased platelet size and proportion of young platelets correlate with changes in other platelet parameters, we quantified levels of receptors that regulate platelet production and activation. Notably several receptors we focused on, including αIIbβ3, GPIbα, GPVI-FcR γ-chain, CLEC-2 and G6b-B rely on SFKs to transmit signals.[2] Surface levels of integrin αIIb were marginally increased in *DKO* platelets, whereas GPIbα

levels were increased by 63% and 38% in *Csk KO* and *DKO* platelets, respectively (Figure 1Di). Surface levels of GPVI were reduced by 77%, 44% and 88% in *Csk KO*, *CD148 KO* and *DKO* platelets, respectively, correlating with total protein levels of GPVI and FcR γ-chain (Figure 1Di-ii). Surface and total protein levels of CLEC-2 were reduced in *Csk KO* and *DKO* platelets, which were significantly more pronounced in *DKO* (Figure 1Di-ii). In contrast, surface expression of the inhibitory receptor G6b-B was increased by 61% and 73% in *Csk KO* and *DKO* platelets, respectively, correlating with total protein levels (Figure 1Di-ii). Surface levels of the integrin α2 subunit and metalloproteinase ADAM10 that mediates shedding of GPVI were normal (Figure S3A). Intriguingly, expression of surface receptors in αIIb^+ bone marrow cells was normal in all three genotypes (Figure S3B), suggesting auto-regulation of these receptors in platelets. Collectively, these findings demonstrate downregulation of the (hemi-)ITAM-containing activation receptors GPVI-FcR γ-chain and CLEC-2, and concomitant upregulation of the ITIM-containing inhibitory receptor G6b-B in Csk-deficient platelets.

To investigate the cause of low platelet counts, we measured the rate of platelet recovery following anti-GPIbα antibody-mediated platelet depletion. This was significantly reduced in *Csk KO* mice, marginally reduced in *CD148 KO* and normal in *DKO* mice (Figure 1Ei-ii). The clearance of biotinylated platelets was normal in mice of all three genotypes (Figure S4A-B). Both *Csk KO* and *DKO* mice exhibited splenomegaly (Figure S5A-B). Elevated MK counts were observed in spleens in all three genotypes, which was associated with myelofibrosis (Figure S6A). MK counts were moderately elevated in the bone marrow of *Csk KO* mice, but with no associated myelofibrosis (Figure S6B). We observed more P-$selectin^+\alpha IIb^+$ hematopoietic cells in *Csk KO* and *DKO* mice (Figure S6C), which may

explain the presence of myelofibrosis in the spleen of these mice.[44] Together, these findings suggest defective MK activation in *Csk KO* and *DKO* mice.

Hemostatic and thrombotic defects in Csk/CD148-deficient platelets

We hypothesized that *Csk KO* mice would be predisposed to thrombosis, due to increased SFK activity, rendering platelets hyperactive. To test this, we analyzed mice of all three genotypes in established *in vivo* models of hemostasis and thrombosis. Paradoxically, *Csk KO* mice exhibited increased bleeding in a tail injury model (Figure 2A). *CD148 KO* mice exhibited normal hemostasis, whereas *DKO* mice had increased bleeding compared to *Csk KO* mice (Figure 2A). Increased bleeding in *Csk KO* and *DKO* mice could not be explained solely by reduced platelet count, which was normal in *DKO* mice.

To explore the kinetics of arterial thrombus formation, we employed the laser injury-induced thrombosis model in small arterioles in mice. Thrombus formation and fibrin deposition were moderately and severely reduced in *Csk KO* and *DKO* mice, respectively (Figure 2Bi-iv and Videos 1-2). Thrombus formation was also severely compromised in *CD148 KO* mice, whereas fibrin deposition was only moderately reduced (Figure 2Bi-iv). Similar results were observed following $FeCl_3$-induced injury of the carotid artery, albeit thrombus formation was marginally better in *CD148 KO* compared with *Csk KO* mice (Figure 2Ci-iii and Video 3). These results demonstrate that the ability of *Csk KO* and *DKO* mice to form thrombi *in vivo* is markedly reduced, resulting in increased bleeding.

Aberrant platelet function underlies thrombotic and defects

To determine the cause of reduced thrombus formation observed in the different *in vivo* models, we employed the T-TAS microfluidic device, which can differentiate between platelet- and coagulation-driven defects. We found that platelets of all three genotypes

displayed severe defects in forming stable platelet thrombi on collagen surface, as we were unable to detect an increase in the flow pressure (Figure 3Ai). However, under conditions where platelets were flowed over collagen in the presence of tissue factor to maximize coagulation, platelets of all three genotypes formed equally stable thrombi (Figure 3Aii), suggesting coagulation is unaltered in these mice and that defects in thrombus formation are intrinsic to platelets.

To identify specific platelet defects, we measured multiple parameters of platelet function and thrombus formation *ex vivo* at arterial shear rates on collagen I, von Willebrand factor-binding peptide (vWF-BP) and laminin, and vWF-BP, laminin and the snake venom rhodocytin, which induces CLEC-2 signaling. We found markedly decreased platelet deposition and thrombus formation on collagen I in *Csk KO* and *CD148 KO* samples, which were further reduced in *DKO* samples (Figure 3Bi-iii and vi). α-granule secretion, integrin αIIbβ3 activation and phosphatidylserine (PS) exposure (determined as P-selectin, JON/A and Annexin V staining, respectively) followed the same trends (Figure 3Biv-vi). This likely is a consequence of markedly reduced surface levels of GPVI-FcR γ-chain, defective SFK signaling and increased inhibitory mechanisms. We found no difference between genotypes in platelet deposition on the vWF-BP and laminin surface on which adhesion is mediated by platelet GPIbα via immobilized plasma vWF and platelet integrin α6β1, which binds laminin,[45] suggesting Csk and CD148 do not play major roles regulating GPIbα or α6β1 signaling pathways (Figure 3Bi-ii and vi). Upon complementing the vWF-BP and laminin surface with the CLEC-2 ligand rhodocytin, which drives a more robust platelet deposition,[46] adhesion was significantly reduced in the three *KOs* (Figure 3Bi-ii, vi). Notably, CLEC-2 expression was marginally and markedly reduced in *Csk KO* and *DKO* platelets, respectively,

demonstrating that Csk and CD148 participate in SFK regulation during CLEC-2-evoked hemi-ITAM signaling, as previously described.[32]

We next analyzed platelets of all three genotypes in a range of *in vitro* functional assays. Consistent with previous findings, *CD148 KO* platelets exhibited reduced aggregation and ATP secretion to collagen and CRP stimulation, which was overcome at high concentrations of CRP (Figure 3Ci-ii). *Csk KO* and *DKO* platelets also exhibited reduced reactivity to collagen, and failed to respond to collagen-related peptide (CRP) (Figure 3Ci-ii). We also investigated the aggregation and ATP secretion response of platelets to anti-CLEC-2 antibody-mediated activation. *CD148 KO* platelets exhibited an increase in the lag time at low concentration of anti-CLEC-2 antibody, and responded normally to a high concentration (Figure 3Ciii). In contrast, *Csk KO* and *DKO* platelets exhibited shortened lag times in response to anti-CLEC-2 antibody, despite expressing lower levels of CLEC-2 receptor (Figures 1Di-ii and 3Ciii). Platelets from all three mouse models responded normally to thrombin and TxA_2 analogue U46619 (Figure 3Civ-v). As expected, *WT* platelets prepared in the absence of apyrase did not respond to 10 μM ADP, due to $P2Y_1$ and $P2Y_{12}$ receptor desensitization (Figure 3Cvi); however, *Csk KO* and *DKO* platelets were able to aggregate and secrete ATP in response to the same concentration of ADP (Figure 4Cvi), suggesting reduced $P2Y_1$ and $P2Y_{12}$ internalization or increased signaling via these receptors, both of which utilize SFKs to transmit signals.[2] Indeed, washed platelets prepared in the presence of apyrase, preventing receptor desensitization, responded normally to 3 and 10 μM ADP, except for *DKO* platelets, which hyper-responded (Figures 3Cvii and S7), supporting the hypothesis of increased $P2Y_{12}$ signaling.

We investigated platelet adhesion and spreading on fibrinogen, which is dependent on SFK-mediated αIIbβ3 outside-in signaling and cytoskeletal remodeling. As expected, Csk-deficient platelets spread to a greater extent than *WT* platelets, whereas CD148-deficient

platelets exhibited reduced spreading (Figure 3Di-ii). However, *DKO* platelets spread comparably to *WT* platelets, suggesting that negative feedback mechanisms were activated in *DKO* platelets. When platelets were pre-activated with thrombin, spreading of *Csk KO* and *DKO* platelets were significantly increased compared to *WT* (Figure 3Di-ii).

To further test the role of Csk and CD148 in αIIbβ3 signaling, we assessed clot retraction in these mice *in vitro*, revealing a significant reduction in clot retraction of *CD148 KO* platelets (Figure 3E). These results strongly suggest an important role for functional Src kinase activity in clot retraction.

Increased SFK activity in Csk/CD148-deficient platelets

To determine the mechanism underlying the hypo-thrombotic phenotypes, we assessed SFK activity in unstimulated platelets of all three genotypes. We measured *trans*-auto-phosphorylation of the activation loop tyrosine residue of SFKs (Src p-Tyr418) as an indirect indicator of SFK activity in resting platelets by quantitative capillary electrophoresis-based immunoassays (ProteinSimple Wes). As expected, deletion of Csk resulted in a significant increase in Src p-Tyr418, whereas deletion of CD148 resulted in a marked decrease in Src p-Tyr418 (Figure 4Ai-ii). Deletion of both Csk and CD148 resulted in an unexpected overall increase in Src p-Tyr418, demonstrating high activity SFKs in these platelets (Figure 4Ai-ii and B).

Phosphorylation of the C-terminal inhibitory tyrosine residues of Lyn (Tyr507), Src (Tyr529) and Fyn (Tyr530) is typically inversely related to SFK activity and to Src p-Tyr418. Indeed, phosphorylated Lyn Tyr507 (Lyn p-Tyr507) was not detected in resting Csk-deficient platelets (Figure 4Ai-ii), and phosphorylation of Src Tyr529 (Src p-Tyr529) and Fyn Tyr530 (Fyn p-Tyr530) were markedly decreased, suggesting that Csk is the main kinase that phosphorylates these residues and attenuates the activity of these SFKs. Conversely,

phosphorylation of all three inhibitory tyrosine residues was increased in resting CD148-deficient platelets (Figure 4Ai-ii), confirming previous findings that CD148-induced dephosphorylation activates SFKs in platelets.[31] A partial rescue of Lyn p-Tyr507, Src p-Tyr529 and Fyn p-Tyr530 was observed in *DKO* platelets (Figure 4Ai-ii), suggesting that in the absence of Csk and CD148 another kinase phosphorylates these residues, the obvious candidate being Chk, which was upregulated in *Csk KO* and *DKO* platelets (Figure 4C), explaining the rescue of inhibitory site phosphorylation of SFKs in *DKO* platelets. Expression of the tyrosine phosphatases PTP-1B, Shp1 and Shp2, all of which have been implicated in regulating SFK activity were normal in all three genotypes (Figure 4C). Interestingly, SFK activity (Src p-Tyr418) was highest in *DKO* platelets, despite increased phosphorylation of the C-terminal inhibitory tyrosine residues of Lyn, Src and Fyn, compared with *Csk KO* platelets. It remains to be determined whether phosphorylation of the activation loop and C-terminal inhibitory tyrosine residues co-exist in the same molecules or in distinct pools of SFKs. Dually phosphorylated SFKs have been reported to be active in T cells.[47]

We next assessed whether SFK activity in MKs is comparable to platelets. Indeed, SFKs were similarly phosphorylated in starved BM-derived MKs (Figure S8A-B) as they were in resting platelets of the same genotype (Figure 4Ai-ii), compatible with increased SFK activity in *Csk KO* and *DKO* MKs, and decreased SFK activity in *CD148 KO* MKs, which may underlie aberrant MK function and myelofibrosis in *Csk KO* and *DKO* mice.

Collectively, these findings demonstrate that Csk is an inhibitor of SFK activity in platelets and MKs. The finding that *DKO* platelets display markedly elevated SFK activity compared to *Csk KO* platelets suggest that CD148 can act as a dual activator and inhibitor of SFK activity in platelets and MKs (Figure 4B).

ITAM and integrin receptor signaling is differentially regulated by Csk and CD148

To determine why platelets with high SFK activity were hypo-reactive, we investigated tyrosine phosphorylation downstream of GPVI-FcR γ-chain, CLEC-2 and αIIbβ3, all of which rely on SFKs and Syk to initiate and propagate signaling. Due to the dramatic reduction of GPVI-FcR γ-chain expression in *Csk KO* and *DKO* platelets (Figure 1Di-ii), platelets were stimulated with a high concentration of collagen (30 μg/ml), which signals primarily through GPVI-FcR γ-chain. Basal whole cell tyrosine phosphorylation (p-Tyr) and Src p-Tyr418 were significantly increased in resting *DKO* platelets and collagen-stimulated *Csk KO* and *DKO* platelets compared with *WT* platelets (Figure 5Ai-iii and S9A). In contrast, basal and collagen-mediated Src p-Tyr418 was significantly reduced in *CD148 KO* platelets compared with *WT* platelets (Figure 5Ai-iii and S9A). Induced phosphorylation of the FcR γ-chain, which is directly mediated by SFKs and acts as a docking site for Syk, was less pronounced in *Csk KO* and *DKO* platelets (Figure 5Ai) due to reduced expression of the FcR γ-chain in these platelets (Figure 1Dii). Syk activation was indirectly measured as phosphorylation of Syk tyrosine residues 525 and 526 (Syk p-Tyr525/6), and correlated directly with FcR γ-chain levels and phosphorylation. Syk p-Tyr525/6 was highest in collagen-stimulated *WT* platelets, and increased only marginally in collagen-stimulated platelets of all three genotypes (Figure 5Aii-iii and S9A), despite *Csk KO* and *DKO* platelets having high SFK activity. These findings support a model in which receptor-mediated membrane localization of Syk is essential for activation.

Platelets were also stimulated with a high concentration of anti-CLEC-2 antibody (10 μg/ml), mimicking podoplanin-mediated cross-linking of the receptor. The pattern and intensity of whole cell p-Tyr and SFK phosphorylation generally mirrored that of collagen-stimulation in the various genotypes (Figure 5Bi-iii and S9B). However, Syk p-Tyr525/6 was much higher in *Csk KO* platelets compared with any of the other genotypes (Figure 5Bii-

iii and S9B), despite reduced CLEC-2 expression. Despite the reduced CLEC-2 and GPVI-FcR γ-chain levels in *DKO* platelets, stimulation by anti-CLEC-2 antibody resulted in normal Syk p-Tyr525/6, whereas stimulation by collagen led to significantly reduced Syk phosphorylation, correlating with normal and reduced aggregation, respectively.

We also investigated αIIbβ3 signaling to determine the cause of increased spreading of *Csk KO* platelets on fibrinogen (Figure 3Di-ii). To initiate signaling, αIIbβ3 relies mainly on Src, and to a lesser extent Fyn and is localized exclusively in non-lipid rafts.[8,15,48,49] Whole cell p-Tyr was increased in fibrinogen-adhered *Csk KO* and *DKO* platelets (Figure 5Ci), demonstrating a general increase in outside-in integrin signaling in these platelets. In agreement with increased spreading of *Csk KO* platelets, but normal spreading of *DKO* platelets on fibrinogen (Figure 3Di-ii, basal), we found increased SFK and Syk activities in *Csk KO* platelets, but not significantly higher SFK and Syk activities in *DKO* platelets (Figure 5Cii-iv and S9C).

In addition to the elevated expression of the ITIM-containing receptor G6b-B in *Csk KO* and *DKO* platelets (Figure 1Di-ii), we found a marked increase in G6b-B tyrosine phosphorylation and binding of the tyrosine phosphatases Shp1 and Shp2 under resting and collagen-stimulated conditions (Figure 5Di), suggesting increased inhibitory signaling via the G6b-B-Shp1-Shp2 complex in *Csk KO* and *DKO* platelets (Figure 5Dii). Thus, increased SFK activity in *Csk KO* and *DKO* platelets leads to compensatory upregulation of inhibitory ITIM signaling and parallel downregulation of the (hemi-)ITAM-containing GPVI-FcR γ-chain and CLEC-2 receptors, explaining the reduced activity of these platelets.

Csk is a critical inhibitor of ITAM- and integrin-mediated platelet activation

To circumvent developmental and compensatory mechanisms arising from deletion of Csk, we utilized a transgenic mouse model expressing a PP1-analogue (3-IB-PP1) sensitive form of Csk (*Csk*^{AS}), enabling rapid and specific inhibition of *Csk*^{AS} in these mice.[39] Platelet count, volume and receptor expression were normal in *Csk*^{AS} mice (*data not shown*). Platelets from *Csk*^{AS} mice aggregated and secreted normally to all agonists tested in the presence of vehicle alone (dimethyl sulfoxide, DMSO) (Figure 6Ai-iv), and marginally more robustly to a sub-threshold concentration of anti-CLEC-2 antibody (3 μg/ml) in the presence of 10 μM 3-IB-PP1 (Figure 6Aiii). Inhibitor-treated *Csk*^{AS} platelets also spread marginally better than control on fibrinogen (Figure 6Bi-ii). Collectively, these findings validate that Csk is an inhibitor of both ITAM and integrin receptor mediated platelet functions. SFK activity (Src p-Tyr418) was significantly increased in resting, CRP (30 μg/ml) and anti-CLEC-2 antibody (10 μg/ml) stimulated *Csk*^{AS} platelets treated with 10 μM 3-IB-PP1 (Figures 6Ci-iii, Di-iii and S10A-B). However, Lyn p-Tyr507, Src p-Tyr529 and Fyn p-Tyr530 were only minimally reduced in the presence of 3-IB-PP1 (Figure 6Cii-iii, Dii-iii and S10A-B), suggesting that tyrosine phosphatases do not automatically dephosphorylate these residues in the absence of Csk. Syk activity was significantly increased at later time points post CRP-stimulation (Figure 6Cii-iii and S10A). Concomitantly, G6b-B was hyper-phosphorylated and had more associated Shp1 and Shp2 in collagen-stimulated *Csk*^{AS} platelets treated with 3-IB-PP1 (Figure 6E). As *G6b-B KO* platelets display markedly elevated Syk activity,[28] we hypothesized that the increased inhibitory signaling provided by G6b-B impeded further enhancement of CRP- and CLEC-2 antibody-mediated aggregation and overall tyrosine phosphorylation in *Csk*^{AS} platelets. These findings suggest that SFKs activate inhibitory pathways in parallel with activation pathways, to prevent platelet hyper-activation.

Discussion

Here we describe a fundamental mechanism controlling SFK activity in the MK lineage, involving the kinase Csk, and the phosphatase CD148. We show that Csk is a major inhibitor of SFKs in platelets, whereas CD148 primarily activates SFKs, but also attenuates SFK activity under as yet undefined conditions (Figures 4B and 7A). These functions of Csk and CD148 correlate with what has previously been described in immune cells.[31,50-55] We show that lack of Csk in the MK lineage in mice results in increased SFK activity in platelets, paradoxical bleeding and reduced thrombosis due to negative feedback mechanisms, including downregulation of (hemi-)ITAM-containing receptors, and concomitant upregulation of the inhibitory ITIM-containing receptor G6b-B rendering platelets less responsive to vascular injury (Figure 7B). In contrast, deletion of CD148 results in reduced SFK activity and thrombus formation as a consequence of reduced (hemi-)ITAM and integrin receptor signaling. Bleeding was however normal in *CD148 KO* mice due to residual SFK activity and intact positive feedback mechanisms. Intriguingly, deletion of both Csk and CD148 markedly increased SFK activity, with more pronounced bleeding and thrombotic defects than in *Csk KO* mice, due to enhanced negative feedback effects (Figure 7B). A summary of the phenotypes of *Csk KO*, *CD148 KO* and *DKO* mice is provided in Table 1. Thus, sustained high SFK activity in platelets does not culminate in a general increase in platelet reactivity, but overcompensation of negative feedback mechanisms that attenuate the platelet response to various thrombogenic substrates. Moreover, reduced platelet count in *Csk KO* mice was not due to increased platelet clearance, but rather a reduction in platelet production, agreeing with a lack of activation and phagocytosis markers on platelets in these mice. Although mean platelet count was rescued in *DKO* mice, the variability in count, platelet volume and the proportion of reticulated platelets in the circulation suggested a less robust system controlling platelet homeostasis in the absence of Csk and CD148.

Negative feedback mechanisms activated in the *Csk KO* and *DKO* mice, including downregulation of the (hemi-)ITAM-containing receptors GPVI-FcR γ-chain and CLEC-2, and upregulation of the ITIM-containing receptor G6b-B and tyrosine kinase Chk, likely represent cell-intrinsic adaptation of platelets to high SFK activity. These findings are in agreement with the reduction of the ITAM-containing T cell receptor in Csk-deficient T cells,[56] and increased phosphorylation of the ITIM-containing receptor Sirpα, the lipid phosphatase SHIP1 and Shp1 following inhibition of Csk^{AS} in immune cells.[57] A plausible explanation for the downregulation of (hemi-)ITAM-containing receptors is that these receptors are direct substrates of CD148; similarly, the ITAM-containing T cell receptor subunit CD3 ζ-chain is suggested to be a substrate of the tyrosine phosphatase CD45.[58,59] A clear difference was observed in the downregulation of GPVI-FcR γ-chain and CLEC-2, suggesting differential regulation of these receptors. Whereas the GPVI-FcR γ-chain was severely reduced in both *Csk KO* and *DKO* platelets, CLEC-2 was markedly downregulated only in *DKO* platelets. This may be explained by the different affinities of Syk to different phospho-(hemi-)ITAMs,[60,61] and thus the ability of the SH2 domains of Syk to protect tyrosine residues within these motifs from dephosphorylation by CD148, as proposed for the related kinase ZAP-70.[62-64] We hypothesize, that the higher affinity of the tandem SH2 domains of Syk for the dual phospho-tyrosine residues of the FcR γ-chain ITAM in *Csk KO* platelets prevents CD148-mediated dephosphorylation. Sustained phosphorylation would in turn lead to internalization and degradation of the GPVI-FcR γ-chain complex. In contrast, due to the lower binding affinity of individual SH2 domains of Syk for single phospho-tyrosine residues with the hemi-ITAM of CLEC-2, Syk is less capable of protecting CLEC-2 from dephosphorylation by CD148. As a consequence, less CLEC-2 is destined for degradation than FcR γ-chain in *Csk KO* platelets. This is not however the case in *DKO*

platelets where no CD148 is present to dephosphorylate CLEC-2, hence it is markedly downregulated. Further work is needed to validate this hypothesis.

Analysis of tyrosine phosphorylation downstream of GPVI, CLEC-2 and αIIbβ3 revealed that activation of Syk is not only dependent on SFK activity, but also on the presence of appropriate docking sites at the plasma membrane, providing evidence that increased SFK activity alone is insufficient to initiate downstream signaling. A growing body of evidence has established G6b-B as a major inhibitor of (hemi-)ITAM-containing receptor signaling in platelets, acting primarily at the level of Syk.[28,65] It is therefore likely that increased G6b-B expression, phosphorylation, and Shp1 and Shp2 association contributes to the attenuation of (hemi-)ITAM signaling in *Csk KO* and *DKO* platelets. Upregulation of Chk in the absence of Csk likely also contributes to the attenuation of SFK-mediated signaling in these platelets, albeit less efficiently than it's structurally related counterpart Csk. Although, Chk was previously reported in platelets,[66] it was not detected in either human or mouse platelets by mass spectrometry,[3,4] in agreement with our findings from *WT* platelets. Thus, the combination of reduced (hemi-)ITAM-containing receptor expression combined with increased ITIM-containing receptor and Chk expression result in a reduction in platelet reactivity to specific substrates. This is better tolerated than pre-activated platelets that can trigger disseminated intravascular coagulation and death.

To circumvent masking effects of negative feedback mechanisms in *Csk KO* or *DKO* mice, we utilized *Csk*^{AS} mice. Inhibition of Csk^{AS} in platelets from these mice, resulted in significantly reduced phosphorylation of the C-terminal inhibitory tyrosine residues of SFKs, and increased SFK and Syk activity, similar to that reported in immune cells.[39,57,67] However, inhibition of Csk^{AS} in platelets failed to have an effect on platelet aggregation. This can be partially explained by increased formation of the G6b-B-Shp1-Shp2 complex, counter-acting the effect of increased SFK activity on Syk activation.[25,28] Our findings also suggest that Csk

plays little role in attenuating GPVI and CLEC-2 signaling once initiated, mainly providing a break prior to ligand engagement and receptor clustering to prevent unwanted signaling by the receptors. This was not however the case for αIIbβ3-mediated platelet spreading on fibrinogen, which was enhanced either in the absence of Csk or following inhibition of Csk^{AS}, suggesting Csk differentially regulates integrin and ITAM-containing receptor signaling. Previous work from our group suggests that G6b-B facilitates rather than inhibits integrin-mediated responses in platelets and MKs,[28] thus upregulation of the G6b-B-Shp1-Shp2 complex is predicted to enhance rather than attenuate platelet spreading, as observed.

In addition to filling a major gap in our knowledge of how SFKs are regulated in the MK lineage, findings from this study are also clinically relevant, demonstrating for the first time that either increased or decreased platelet SFK activity can lead to reduced thrombus formation and bleeding. Our study highlights, that loss of an inhibitor of platelet activation, such as Csk, can lead to paradoxical bleeding due to the robust negative feedback mechanisms that get activated. This may provide important mechanistic insights into the phenomenon of early platelet dysfunction observed in severe trauma patients displaying 'exhausted' platelets,[68] showing reduced thrombus formation on collagen.[69] Our findings that platelets in the circulation can undergo cell-intrinsic changes, leading to downregulation of activation pathways and upregulation of inhibitory mechanisms may contribute to platelet dysfunction in trauma patients. Moreover, certain tyrosine kinase inhibitors used to treat cancer patients inhibit SFKs or Csk and are accompanied with bleeding side-effects. Accordingly, the increased bleeding risk associated with use of the Bcr-Abl inhibitor Dasatinib is ascribed to its off-target effects on platelet SFKs.[70,71] Similarly, bleeding-side effects of the Btk inhibitor Ibrutinib may be partially explained by its potent off-target effect on Csk.[72,73] Based on our findings, CD148 is an attractive anti-thrombotic drug target, inhibition of which should attenuate, but not completely block any of the main platelet

activation pathways and have minimal bleeding side-effects. Tyrosine phosphatases are increasingly considered to be druggable,[74] supported by the recent development of the highly specific Shp2 inhibitor SHP099,[75] thus targeting CD148 is not inconceivable.

Acknowledgements

JM and ZN are British Heart Foundation (BHF) postdoctoral research associates, AM is a BHF Intermediate Basic Science Research Fellow (FS/15/58/31784) and YAS is a BHF Senior Basic Science Research Fellow (FS/13/1/29894). RA was supported by the government of the Sultanate of Oman. This work was supported by BHF Project Grant PG/11/108/29237 and Programme Grant RG/15/13/31673. We thank Timo Vögtle for critical reading of the manuscript and invaluable discussions, Quadratech Diagnostics for providing the T-TAS device, and all members of the Birmingham Biomedical Sciences Unit for maintenance of mouse colonies.

Authorship Contributions

Conceptualization: JM, ZN, AM and YAS; Methodology: JM, ZN, JWMH, AM and YAS; Formal Analysis: JM, ZN, CWS, RA, JPG, BMET, GEJ, AM and YAS; Investigation: JM, ZN, GDN, CWS, MJG, RA, JPG, SH, LB, JNC, LT, MJEK, PH, JWMH, AM and YAS; Resources: YAS; Mouse models and reagents: AT and AW; Equipment and expertise: PH; Writing: JM, ZN, AM, and YAS; Revising and editing: JM, ZN, JWMH, GEJ, AW, AM and YAS; Supervision: AM and YAS

Conflict of Interest Disclosures

The authors declare no competing financial interests.

References

1. Golden A, Nemeth SP, Brugge JS. Blood platelets express high levels of the pp60c-src-specific tyrosine kinase activity. *Proc Natl Acad Sci U S A*. 1986;83(4):852-856.

2. Senis YA, Mazharian A, Mori J. Src family kinases: at the forefront of platelet activation. *Blood*. 2014;124(13):2013-2024.

3. Burkhart JM, Vaudel M, Gambaryan S, et al. The first comprehensive and quantitative analysis of human platelet protein composition allows the comparative analysis of structural and functional pathways. *Blood*. 2012;120(15):e73-82.

4. Zeiler M, Moser M, Mann M. Copy number analysis of the murine platelet proteome spanning the complete abundance range. *Mol Cell Proteomics*. 2014;13(12):3435-3445.

5. Ezumi Y, Shindoh K, Tsuji M, Takayama H. Physical and functional association of the Src family kinases Fyn and Lyn with the collagen receptor glycoprotein VI-Fc receptor gamma chain complex on human platelets. *J Exp Med*. 1998;188(2):267-276.

6. Quek LS, Pasquet JM, Hers I, et al. Fyn and Lyn phosphorylate the Fc receptor gamma chain downstream of glycoprotein VI in murine platelets, and Lyn regulates a novel feedback pathway. *Blood*. 2000;96(13):4246-4253.

7. Arias-Salgado EG, Lizano S, Sarkar S, Brugge JS, Ginsberg MH, Shattil SJ. Src kinase activation by direct interaction with the integrin beta cytoplasmic domain. *Proc Natl Acad Sci U S A*. 2003;100(23):13298-13302.

8. Reddy KB, Smith DM, Plow EF. Analysis of Fyn function in hemostasis and alphaIIbbeta3-integrin signaling. *J Cell Sci*. 2008;121(Pt 10):1641-1648.

9. Schmaier AA, Zou Z, Kazlauskas A, et al. Molecular priming of Lyn by GPVI enables an immune receptor to adopt a hemostatic role. *Proc Natl Acad Sci U S A*. 2009.

10. Maxwell MJ, Yuan Y, Anderson KE, Hibbs ML, Salem HH, Jackson SP. SHIP1 and Lyn Kinase Negatively Regulate Integrin alpha IIb beta 3 signaling in platelets. *J Biol Chem*. 2004;279(31):32196-32204.

11. Falati S, Edmead CE, Poole AW. Glycoprotein Ib-V-IX, a receptor for von Willebrand factor, couples physically and functionally to the Fc receptor gamma-chain, Fyn, and Lyn to activate human platelets. *Blood*. 1999;94(5):1648-1656.

12. Ozaki Y, Asazuma N, Suzuki-Inoue K, Berndt MC. Platelet GPIb-IX-V-dependent signaling. *J Thromb Haemost*. 2005;3(8):1745-1751.

13. Suzuki-Inoue K, Tulasne D, Shen Y, et al. Association of Fyn and Lyn with the proline-rich domain of glycoprotein VI regulates intracellular signaling. *J Biol Chem*. 2002;277(24):21561-21566.

14. Fox JE, Lipfert L, Clark EA, Reynolds CC, Austin CD, Brugge JS. On the role of the platelet membrane skeleton in mediating signal transduction. Association of GP IIb-IIIa, pp60c-src, pp62c-yes, and the p21ras GTPase-activating protein with the membrane skeleton. *J Biol Chem*. 1993;268(34):25973-25984.

15. Obergfell A, Eto K, Mocsai A, et al. Coordinate interactions of Csk, Src, and Syk kinases with [alpha]IIb[beta]3 initiate integrin signaling to the cytoskeleton. *J Cell Biol*. 2002;157(2):265-275.

16. Murugappan S, Shankar H, Bhamidipati S, Dorsam RT, Jin J, Kunapuli SP. Molecular mechanism and functional implications of thrombin-mediated tyrosine phosphorylation of PKCdelta in platelets. *Blood*. 2005;106(2):550-557.

17. Li Z, Zhang G, Liu J, et al. An important role of the SRC family kinase Lyn in stimulating platelet granule secretion. *J Biol Chem*. 2010;285(17):12559-12570.

18. Kim S, Kunapuli SP. Negative regulation of Gq-mediated pathways in platelets by G(12/13) pathways through Fyn kinase. *J Biol Chem*. 2011;286(27):24170-24179.

19. Xiang B, Zhang G, Stefanini L, et al. The Src family kinases and protein kinase C synergize to mediate Gq-dependent platelet activation. *J Biol Chem*. 2012;287(49):41277-41287.

20. Hardy AR, Jones ML, Mundell SJ, Poole AW. Reciprocal cross-talk between P2Y1 and P2Y12 receptors at the level of calcium signaling in human platelets. *Blood*. 2004;104(6):1745-1752.

21. Nash CA, Severin S, Dawood BB, et al. Src family kinases are essential for primary aggregation by G(i) -coupled receptors. *J Thromb Haemost*. 2010;8(10):2273-2282.

22. Poole A, Gibbins JM, Turner M, et al. The Fc receptor gamma-chain and the tyrosine kinase Syk are essential for activation of mouse platelets by collagen. *Embo J*. 1997;16(9):2333-2341.

23. Coxon CH, Geer MJ, Senis YA. ITIM receptors: more than just inhibitors of platelet activation. *Blood*. 2017;129(26):3407-3418.

24. Hua CT, Gamble JR, Vadas MA, Jackson DE. Recruitment and activation of SHP-1 protein-tyrosine phosphatase by human platelet endothelial cell adhesion molecule-1 (PECAM-1). Identification of immunoreceptor tyrosine-based inhibitory motif-like binding motifs and substrates. *J Biol Chem*. 1998;273(43):28332-28340.

25. Mazharian A, Mori J, Wang YJ, et al. Megakaryocyte-specific deletion of the protein-tyrosine phosphatases Shp1 and Shp2 causes abnormal megakaryocyte development, platelet production, and function. *Blood*. 2013;121(20):4205-4220.

26. Jackson DE, Ward CM, Wang R, Newman PJ. The protein-tyrosine phosphatase SHP-2 binds platelet/endothelial cell adhesion molecule-1 (PECAM-1) and forms a distinct signaling complex during platelet aggregation. Evidence for a mechanistic link between PECAM-1- and integrin-mediated cellular signaling. *J Biol Chem*. 1997;272(11):6986-6993.

27. Falati S, Patil S, Gross PL, et al. Platelet PECAM-1 inhibits thrombus formation in vivo. *Blood*. 2006;107(2):535-541.

28. Mazharian A, Wang YJ, Mori J, et al. Mice lacking the ITIM-containing receptor G6b-B exhibit macrothrombocytopenia and aberrant platelet function. *Sci Signal*. 2012;5(248):ra78.

29. Hermiston ML, Xu Z, Weiss A. CD45: a critical regulator of signaling thresholds in immune cells. *Annu Rev Immunol*. 2003;21:107-137.

30. Senis YA, Tomlinson MG, Ellison S, et al. The tyrosine phosphatase CD148 is an essential positive regulator of platelet activation and thrombosis. *Blood*. 2009;113(20):4942-4954.

31. Ellison S, Mori J, Barr AJ, Senis YA. CD148 enhances platelet responsiveness to collagen by maintaining a pool of active Src family kinases. *J Thromb Haemost*. 2010;8(7):1575-1583.

32. Mori J, Wang YJ, Ellison S, et al. Dominant role of the protein-tyrosine phosphatase CD148 in regulating platelet activation relative to protein-tyrosine phosphatase-1B. *Arterioscler Thromb Vasc Biol*. 2012;32(12):2956-2965.

33. Roskoski R, Jr. Src kinase regulation by phosphorylation and dephosphorylation. *Biochem Biophys Res Commun*. 2005;331(1):1-14.

34. Nada S, Okada M, MacAuley A, Cooper JA, Nakagawa H. Cloning of a complementary DNA for a protein-tyrosine kinase that specifically phosphorylates a negative regulatory site of p60c-src. *Nature*. 1991;351(6321):69-72.

35. Davidson D, Chow LM, Veillette A. Chk, a Csk family tyrosine protein kinase, exhibits Csk-like activity in fibroblasts, but not in an antigen-specific T-cell line. *J Biol Chem*. 1997;272(2):1355-1362.

36. Schmedt C, Saijo K, Niidome T, Kuhn R, Aizawa S, Tarakhovsky A. Csk controls antigen receptor-mediated development and selection of T-lineage cells. *Nature*. 1998;394(6696):901-904.

37. Katsumoto TR, Kudo M, Chen C, et al. The phosphatase CD148 promotes airway hyperresponsiveness through SRC family kinases. *J Clin Invest*. 2013;123(5):2037-2048.

38. Tiedt R, Schomber T, Hao-Shen H, Skoda RC. Pf4-Cre transgenic mice allow the generation of lineage-restricted gene knockouts for studying megakaryocyte and platelet function in vivo. *Blood*. 2007;109(4):1503-1506.

39. Tan YX, Manz BN, Freedman TS, Zhang C, Shokat KM, Weiss A. Inhibition of the kinase Csk in thymocytes reveals a requirement for actin remodeling in the initiation of full TCR signaling. *Nat Immunol*. 2014;15(2):186-194.

40. Pearce AC, Senis YA, Billadeau DD, Turner M, Watson SP, Vigorito E. Vav1 and vav3 have critical but redundant roles in mediating platelet activation by collagen. *J Biol Chem*. 2004;279(52):53955-53962.

41. Ohlmann P, Eckly A, Freund M, Cazenave JP, Offermanns S, Gachet C. ADP induces partial platelet aggregation without shape change and potentiates collagen-induced aggregation in the absence of Galphaq. *Blood*. 2000;96(6):2134-2139.

42. Smith CW, Thomas SG, Raslan Z, et al. Mice Lacking the Inhibitory Collagen Receptor LAIR-1 Exhibit a Mild Thrombocytosis and Hyperactive Platelets. *Arterioscler Thromb Vasc Biol*. 2017;37(5):823-835.

43. Pertuy F, Aguilar A, Strassel C, et al. Broader expression of the mouse platelet factor 4-cre transgene beyond the megakaryocyte lineage. *J Thromb Haemost*. 2015;13(1):115-125.

44. Spangrude GJ, Lewandowski D, Martelli F, et al. P-Selectin Sustains Extramedullary Hematopoiesis in the Gata1 low Model of Myelofibrosis. *Stem Cells*. 2016;34(1):67-82.

45. Schaff M, Tang C, Maurer E, et al. Integrin alpha6beta1 is the main receptor for vascular laminins and plays a role in platelet adhesion, activation, and arterial thrombosis. *Circulation*. 2013;128(5):541-552.

46. de Witt SM, Swieringa F, Cavill R, et al. Identification of platelet function defects by multi-parameter assessment of thrombus formation. *Nat Commun*. 2014;5:4257.

47. Nika K, Soldani C, Salek M, et al. Constitutively active Lck kinase in T cells drives antigen receptor signal transduction. *Immunity*. 2010;32(6):766-777.

48. Severin S, Nash CA, Mori J, et al. Distinct and overlapping functional roles of Src family kinases in mouse platelets. *J Thromb Haemost*. 2012;10(8):1631-1645.

49. Arias-Salgado EG, Lizano S, Shattil SJ, Ginsberg MH. Specification of the direction of adhesive signaling by the integrin beta cytoplasmic domain. *J Biol Chem*. 2005;280(33):29699-29707.

50. Pera IL, Iuliano R, Florio T, et al. The rat tyrosine phosphatase eta increases cell adhesion by activating c-Src through dephosphorylation of its inhibitory phosphotyrosine residue. *Oncogene*. 2005;24(19):3187-3195.

51. Stepanek O, Kalina T, Draber P, et al. Regulation of Src family kinases involved in T cell receptor signaling by protein-tyrosine phosphatase CD148. *J Biol Chem*. 2011;286(25):22101-22112.

52. McNeill L, Salmond RJ, Cooper JC, et al. The differential regulation of Lck kinase phosphorylation sites by CD45 is critical for T cell receptor signaling responses. *Immunity*. 2007;27(3):425-437.

53. Zikherman J, Jenne C, Watson S, et al. CD45-Csk phosphatase-kinase titration uncouples basal and inducible T cell receptor signaling during thymic development. *Immunity*. 2010;32(3):342-354.

54. Lin J, Weiss A. The tyrosine phosphatase CD148 is excluded from the immunologic synapse and down-regulates prolonged T cell signaling. *J Cell Biol*. 2003;162(4):673-682.

55. Davis SJ, van der Merwe PA. The kinetic-segregation model: TCR triggering and beyond. *Nat Immunol*. 2006;7(8):803-809.

56. Schmedt C, Tarakhovsky A. Autonomous maturation of alpha/beta T lineage cells in the absence of COOH-terminal Src kinase (Csk). *J Exp Med*. 2001;193(7):815-826.

57. Freedman TS, Tan YX, Skrzypczynska KM, et al. LynA regulates an inflammation-sensitive signaling checkpoint in macrophages. *Elife*. 2015;4.

58. Furukawa T, Itoh M, Krueger NX, Streuli M, Saito H. Specific interaction of the CD45 protein-tyrosine phosphatase with tyrosine-phosphorylated CD3 zeta chain. *Proc Natl Acad Sci U S A*. 1994;91(23):10928-10932.

59. Kashio N, Matsumoto W, Parker S, Rothstein DM. The second domain of the CD45 protein tyrosine phosphatase is critical for interleukin-2 secretion and substrate recruitment of TCR-zeta in vivo. *J Biol Chem*. 1998;273(50):33856-33863.

60. Isakov N, Wange RL, Burgess WH, Watts JD, Aebersold R, Samelson LE. ZAP-70 binding specificity to T cell receptor tyrosine-based activation motifs: the tandem SH2 domains of ZAP-70 bind distinct tyrosine-based activation motifs with varying affinity. *J Exp Med*. 1995;181(1):375-380.

61. Ottinger EA, Botfield MC, Shoelson SE. Tandem SH2 domains confer high specificity in tyrosine kinase signaling. *J Biol Chem*. 1998;273(2):729-735.

62. Iwashima M, Irving BA, van Oers NS, Chan AC, Weiss A. Sequential interactions of the TCR with two distinct cytoplasmic tyrosine kinases. *Science*. 1994;263(5150):1136-1139.

63. Ashe JM, Wiest DL, Abe R, Singer A. ZAP-70 protein promotes tyrosine phosphorylation of T cell receptor signaling motifs (ITAMs) in immature CD4(+)8(+) thymocytes with limiting p56(lck). *J Exp Med*. 1999;189(7):1163-1168.

64. Qian D, Mollenauer MN, Weiss A. Dominant-negative zeta-associated protein 70 inhibits T cell antigen receptor signaling. *J Exp Med*. 1996;183(2):611-620.

65. Coxon CH, Sadler AJ, Huo J, Campbell RD. An investigation of hierachical protein recruitment to the inhibitory platelet receptor, G6B-b. *PLoS One*. 2012;7(11):e49543.

66. Hirao A, Hamaguchi I, Suda T, Yamaguchi N. Translocation of the Csk homologous kinase (Chk/Hyl) controls activity of CD36-anchored Lyn tyrosine kinase in thrombin-stimulated platelets. *Embo J*. 1997;16(9):2342-2351.

67. Manz BN, Tan YX, Courtney AH, et al. Small molecule inhibition of Csk alters affinity recognition by T cells. *Elife*. 2015;4.

68. Wohlauer MV, Moore EE, Thomas S, et al. Early platelet dysfunction: an unrecognized role in the acute coagulopathy of trauma. *J Am Coll Surg*. 2012;214(5):739-746.

69. Li R, Elmongy H, Sims C, Diamond SL. Ex vivo recapitulation of trauma-induced coagulopathy and preliminary assessment of trauma patient platelet function under flow using microfluidic technology. *J Trauma Acute Care Surg*. 2016;80(3):440-449.

70. Quintas-Cardama A, Han X, Kantarjian H, Cortes J. Tyrosine kinase inhibitor-induced platelet dysfunction in patients with chronic myeloid leukemia. *Blood*. 2009;114(2):261-263.

71. Gratacap MP, Martin V, Valera MC, et al. The new tyrosine-kinase inhibitor and anticancer drug dasatinib reversibly affects platelet activation in vitro and in vivo. *Blood*. 2009;114(9):1884-1892.

72. Levade M, David E, Garcia C, et al. Ibrutinib treatment affects collagen and von Willebrand factor-dependent platelet functions. *Blood*. 2014;124(26):3991-3995.

73. Honigberg LA, Smith AM, Sirisawad M, et al. The Bruton tyrosine kinase inhibitor PCI-32765 blocks B-cell activation and is efficacious in models of autoimmune disease and B-cell malignancy. *Proc Natl Acad Sci U S A*. 2010;107(29):13075-13080.

74. Tautz L, Senis YA, Oury C, Rahmouni S. Perspective: Tyrosine phosphatases as novel targets for antiplatelet therapy. *Bioorg Med Chem*. 2015;23(12):2786-2797.

75. Chen YN, LaMarche MJ, Chan HM, et al. Allosteric inhibition of SHP2 phosphatase inhibits cancers driven by receptor tyrosine kinases. *Nature*. 2016;535(7610):148-152.

76. Nieminen P LH, Vähäkangas K, Huusko A, Rautio A. Standardised regression coefficient as an effect size index in summarising findings in epidemiological studies. *Epidemiology Biostatistics and Public Health*. 2013;Volume 10(4):e8854.

Table 1. Summary of *Csk KO*, *CD148 KO* and *DKO* mouse phenotypes.

Phenotype	*Genotype*		
	Csk KO	***CD148 KO***	***DKO***
Bleeding	↑	—	↑↑
Thrombosis			
In vivo			
Laser injury	↓	↓	↓↓
$FeCl_3$ injury	↓↓	↓	↓
Ex vivo			
T-TAS – collagen	↓	↓	↓↓
– collagen, tissue factor	—	—	—
Flow chamber – collagen	↓	↓	↓↓
– vWF-BP, laminin, rhodocytin	↓	↓	↓
Platelet count	↓	—	—
Platelet receptors			
Expression			
GPVI-FcRγ-chain	↓↓	↓	↓↓↓
CLEC-2	↓	—	↓↓
G6b-B	↑↑	—	↑↑
Phosphorylation			
G6b-B	↑↑	—	↑↑↑
SFK activity	↑	↓	↑↑

↑ upregulated, ↓ downregulated, — normal

Figure Legends

Figure 1. Aberrant platelet production and platelet receptor expressions in *Csk KO* mice.

(A) Platelet lysates were blotted for the indicated proteins. (B) Platelet counts. (C) Percentage of reticulated platelets determined by thiazole orange^{+}αIIb^{+} cells in blood. See also Figure S2A. (D) i) Median fluorescence intensity (MFI) measured in αIIb^{+} cells alone or αIIb^{+} cells co-stained for the indicated proteins in blood, n = 5-6 mice/genotype. See also Figure S3. ii) Platelet lysates were blotted for the indicated proteins. (E) i) Platelet counts of pre-/post-injection of anti-GPIbα antibody (1.5 μg/g of body weight). ii) The rate of platelet recovery determined by a proportionate slope from linear trend lines between day 3 to 7 from (i), n = 7-8 mice/genotype. See also Figures S4-6.

Asterisks refer to significant difference compared to *WT*. **P* < 0.05, ****P* < 0.001, one-way ANOVA with Tukey's test (B-D), or one-way ANOVA with Dunnett's test; vs *WT* (E), mean ± SEM.

Figure 2. Increased bleeding and defective thrombus formation in *Csk KO* and *DKO* mice.

(A) Hemostatic response was measured in tail bleeding assays by an excision of a 5-mm portion of the tail tip followed by the determination of lost blood/body weight (normalized blood loss), n = 11-57 mice/genotype. Tail bleeding assays were conducted in a double-blinded manner. (B) Laser injury-induced thrombus formation *in vivo*. Composite brightfield and fluorescence images of i) platelet accumulation (green) or ii) fibrin generation (red) in cremaster muscle arterioles monitored by DyLight488-labaled anti-GPIbβ antibody (0.1 μg/g of body weight) or Alexa-Fluor 647-labeled anti-fibrin antibody (0.2 μg/g of body

weight) signal, respectively by confocal intravital microscopy (scale bar: 10 μm). Each curve represents the median integrated fluorescence intensity of iii) platelets or iv) fibrin in relative fluorescence units (RFU), n = 25-37, in 5 mice/genotype. See also Videos 1 and 2. (C) Ferric chloride injury-induced thrombus formation *in vivo*. Filter paper soaked in 10% ferric chloride was applied to carotid artery for 3 minutes. i) Representative fluorescence images of platelet accumulation (green) monitored by DyLight488-labaled anti-GPIbβ antibody (0.1 μg/g of body weight) by confocal intravital microscopy (scale bar: 200 μm). ii) Each curve represents the median integrated thrombus fluorescence intensity in RFU. iii) Area under the curve (AUC) was measured, n = 8-11 mice per genotype. See also Video 3.

*$P < 0.05$, **$p < 0.01$, ***$p < 0.001$, one-way ANOVA with Tukey's test; mean ± SEM

Figure 3. Aberrant platelet functions in *Csk KO*, *CD148 KO* and *DKO* mice.

(A) i) 25 μg/ml hirudin-treated blood was perfused with collagen-coated chip at 1000 s^{-1} for 10 minutes. Individual time-dependent flow pressure curves and total thrombogenicity (Area under the curve: AUC) were measured by the total thrombus-formation analysis system (T-TAS). ii) Blood treated with 3.2% sodium citrate, 12 mM $CaCl_2$ and 50 μg/ml corn trypsin inhibitor was perfused on collagen plus tissue thromboplastin (tissue factor)-coated chip at 240 s^{-1} for 30 minutes. Individual time-dependent flow pressure curves, time to onset (T10), time to occlusion (T80), rate of thrombus growth (T10-80) and AUC were measured by T-TAS, n = 4-9 per genotype. (B) Blood treated with 5 Unit/ml Heparin, 40 μM PPACK and 50 Unit/ml Fragmin was perfused over microspots with indicated coatings; 100 μg/ml collagen I, 12.5 μg/ml vWF-binding peptide (vWF-BP), 50 μg/ml laminin, 250 μg/ml rhodocytin for 3.5 minutes at 1,000 s^{-1}. i) Representative bright field images with indicated surfaces. ii) Platelet deposition (% surface area coverage; SAC). iii) Multilayered thrombus

(% SAC) on collagen I surface. iv) Representative fluorescence images of P-selectin, integrin αIIbβ3 activation (JON/A) and PS exposure (Annexin V) from collagen surface and v) % SAC of fluorescence images. vi) Heatmap of outcome parameters expressed as effect sizes per genotype;[76] P1, platelet deposition, P2, multilayered thrombus, P3, P-selectin, P4, JON/A, and P5, PS exposure from indicated surfaces. Scale bar: 10 μm. Experiments and analysis were performed in a double-blinded manner. % SAC was analyzed using Fiji programme, n = 15 images from 5 mice per genotype. (C) Representative platelet aggregation and ATP secretion traces in response to the indicated agonists in i-vi) washed platelets or vii) ADP-sensitive washed platelets. See also Figure S7. n = 4-8 mice/condition/genotype. (D) i) Representative differential interference contrast (DIC) microscopy images of resting (basal) and thrombin-stimulated (0.1 Unit/ml, 5 minutes) platelets spread on fibrinogen-coated cover-slips (100 μg/ml, 45 minutes, 37°C, scale bar: 5 μm). ii) Mean surface area of individual platelets quantified by ImageJ software, n = 256 platelets/condition/genotype. (E) Fibrin clot retraction was assessed 2 hours after the addition of 1 Unit/ml thrombin and 2 mM $CaCl_2$ to platelet-rich plasma. Clot volumes were expressed as a percentage of the initial volume of platelet-rich plasma, n = 8 per genotype.
$*P < 0.05$, $**P < 0.01$, $***P < 0.001$, two-way (Bii, Bv, and D) or one-way (A, Biii, and E) ANOVA with Tukey's test, mean ± SEM.

Figure 4. Csk and CD148 reciprocally regulate platelet SFKs.

(A) i) Representative electropherograms of capillary-based immunoassays on platelet lysates with the indicated antibodies and the quantification of peak areas, n = 6 mice/genotype. ii) Representative data from i) displayed as blots. See also Figure S8. (B) Model of SFK regulation in platelets. In *WT* platelets, SFKs are constrained in an inactive conformation by Csk, which phosphorylates the C-terminal inhibitory tyrosine residue. SFKs can be activated

by dephosphorylation of the inhibitory residue by CD148. SFKs *trans*-auto-phosphorylate each other at the activation-loop tyrosine residue and become fully active. CD148 can also dephosphorylate the activation-loop tyrosine leading to a decrease in SFK activity. In *Csk KO* platelets, CD148 dominates resulting in the loss of inhibitory phosphorylation and a net increase in SFK activity. In *CD148 KO* platelets, Csk dominates resulting in increased inhibitory phosphorylation, and markedly decreased activation-loop phosphorylation. In *DKO* platelets, the absence of both Csk and CD148 leads to a dramatic increase in SFK activity. The differential phosphorylation of SFKs in *Csk KO* and *DKO* platelets supports the hypothesis of CD148 dephosphorylating both the activation-loop and the C-terminal inhibitory tyrosine residues. (C) Platelet lysates were blotted for the indicated proteins.
$*P < 0.05$, $**P < 0.01$, $***P < 0.001$, repeated measures (RM) one-way ANOVA with Tukey's test, mean ± SEM.

Figure 5. Csk and CD148 are critical for platelet activation signals.

(A) i) Lysates of basal and collagen-stimulated (30 μg/ml, 90 seconds) platelets were blotted for p-Tyr and tubulin. ii-iii) Same lysates were analyzed by capillary-based immunoassays with the indicated antibodies. ii) Representative data displayed as blots. iii) Quantification of peak areas from Figure S9A , n = 3-4 mice/genotype. See also Figure S9A. (B) i-iii) Lysates of basal and CLEC-2 antibody-stimulated (10 μg/ml, 5 minutes) platelets were analyzed as described in (A), n = 3-4 mice/genotype. See also Figure S9B. (C) i-iii) Lysates of non-adherent (NA) and adherent (Ad) platelets from fibrinogen-coated plates (100 μg/ml, 45 minutes, 37°C) were analyzed as described in (A). See also Figure S9C. iv) Same lysates were blotted for Syk p-Tyr525/6, n = 3-4 mice/genotype. Differences in basal SFK p-Tyr418 between *WT* and *DKO* platelets in suspension (A-B) compared with non-adhered platelets (C), are due to differences in sample preparation, as demonstrated by a significant increase in Src

p-Tyr418 levels in non-adhered platelets incubated on fibrinogen-coated surface (Figure S9D).

(D) i) Increased G6b-B phosphorylation and assembly of the G6b-B-Shp1-Shp2 complex in *Csk KO* and *DKO* platelets. Lysates of basal and collagen-stimulated (30 μg/ml, 90 seconds) platelets were immunoprecipitated with anti-G6b-B antibody and blotted for p-Tyr, G6b-B, Shp1 and Shp2. ii) The role of SFKs in activating and inhibitory pathways. Once a threshold level of SFK activity is reached, ITAM, integrin and ITIM signaling are triggered. The kinetics and order of activation depend upon the agonist and level of SFK activity.

**P* < 0.05, ***P* < 0.01, ****P* < 0.001, RM two-way ANOVA with Tukey's test, mean ± SEM.

Figure 6. Csk regulates ITAM-, ITIM- and integrin-dependent signaling in *Csk*^{AS} platelets.

(A-E) Platelets from *Csk*^{AS} mice were pre-treated with either DMSO or 3-IB-PP1 (10 μM, 10 minutes). (A) i-iv) Representative aggregation and ATP secretion traces of platelets from *Csk*^{AS} mice in response to the indicated agonists, n = 3-4 mice/condition/genotype. (B) i) Representative DIC microscopy images of resting (basal) and thrombin-stimulated (0.1 Unit/ml, 5 minutes) platelets spread on fibrinogen-coated cover-slips (100 μg/ml, 45 minutes, 37°C, scale bar: 5 μm). ii) Mean surface area of individual platelets quantified by ImageJ software, n = 256 platelets/condition/genotype. (C and D) Lysates of platelets incubated with or without CRP (30 μg/ml, C) or CLEC-2 antibody (10 μg/ml, D) for indicated times were i) blotted for p-Tyr and actin, or ii-iii) analyzed by capillary-based immunoassays as described in Figure 5A, n = 3-4 mice/genotype. See also Figure S10A-B. (E) Increased G6b-B phosphorylation and assembly of the G6b-B-Shp1-Shp2 complex in collagen-stimulated *Csk*^{AS} platelets treated with 3-IB-PP1. Lysates of basal and collagen-stimulated (30 μg/ml,

90 seconds) platelets were immunoprecipitated with anti-G6b-B antibody and blotted for p-Tyr, G6b-B, Shp1 and Shp2.

*$P < 0.05$, **$P < 0.01$, ***$P < 0.001$, ordinary (B) or RM (C and D) two-way ANOVA with Sidak's test, mean ± SEM.

Figure 7. Regulation of platelet SFKs by the kinase Csk, and the phosphatase CD148.

(A) Csk and CD148 are the main regulators of SFK activity in platelets and impact on different platelet signaling pathways. Csk inhibits SFK activity, whereas CD148 activates SFKs but it can also inhibit SFK activity under as yet undefined conditions. In turn, SFKs regulate ITAM, integrin, ITIM and $P2Y_{12}$ receptor signaling pathways. See also Figures 4B and 5Dii. (B) Post-activated platelets. Platelets possess remarkable positive-feedback pathways (e.g. ADP, TXA2), which further enhance platelet activation. Platelet activation is followed by receptor proteolysis or internalization, *de novo* protein synthesis and downregulation of tyrosine phosphorylation pathways by ITIM-containing receptors and phosphatases. *Csk KO* and *DKO* platelets have increased SFK activity which results in reduced expression of the platelet activating receptors GPVI and CLEC-2, increased expression of the ITIM-containing receptor G6b-B and increased ITIM signaling suggesting that these platelets exist in a 'post-activated' state.

Figure 1

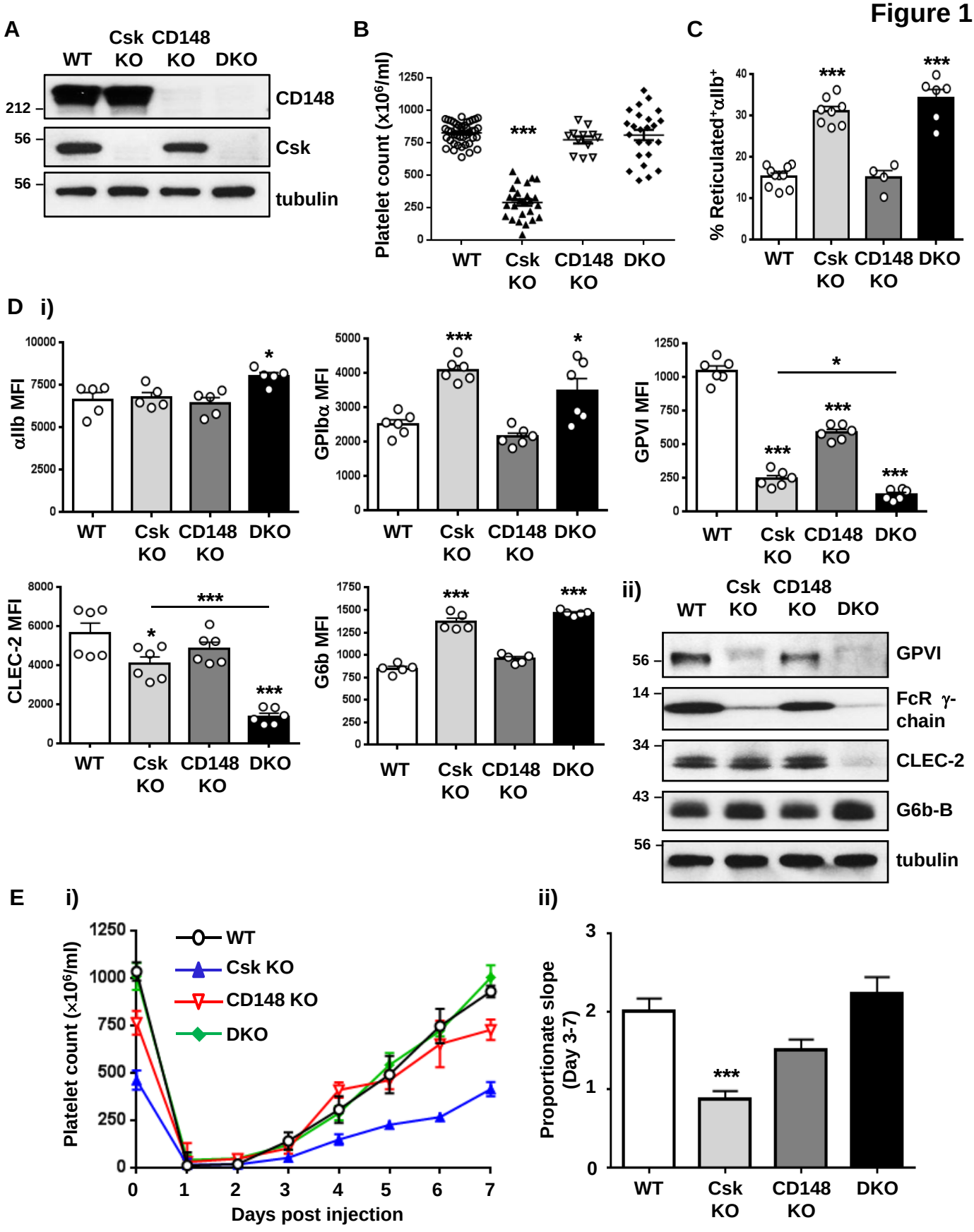
A
WT
Csk KO
CD148 KO
DKO
212
56
56
CD148
Csk
tubulin
B
Platelet count (x10⁶/ml)
C
% Reticulated⁺αIIb⁺
D i)
αIIb MFI
GPIbα MFI
GPVI MFI
CLEC-2 MFI
G6b MFI
ii)
GPVI
FcR γ-chain
CLEC-2
G6b-B
tubulin
E i)
Platelet count (×10⁶/ml)
Days post injection
ii)
Proportionate slope (Day 3-7)

Figure 2

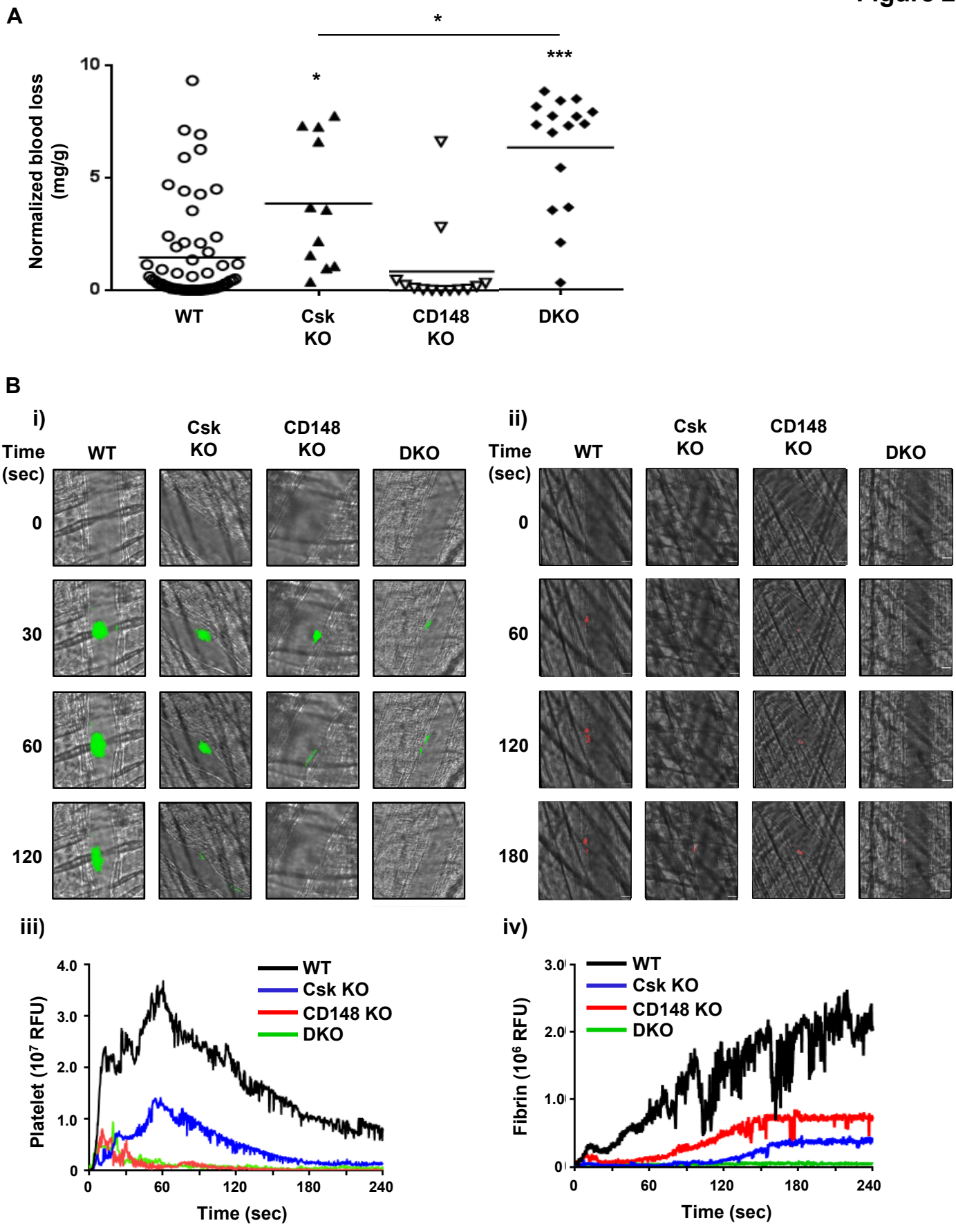
A
*
***
*
Normalized blood loss (mg/g)
10
5
0
WT
Csk KO
CD148 KO
DKO
B
i)
ii)
Time (sec)
WT
Csk KO
CD148 KO
DKO
0
30
60
120
180
iii)
iv)
Platelet (10^7 RFU)
Fibrin (10^6 RFU)
Time (sec)
WT
Csk KO
CD148 KO
DKO

C

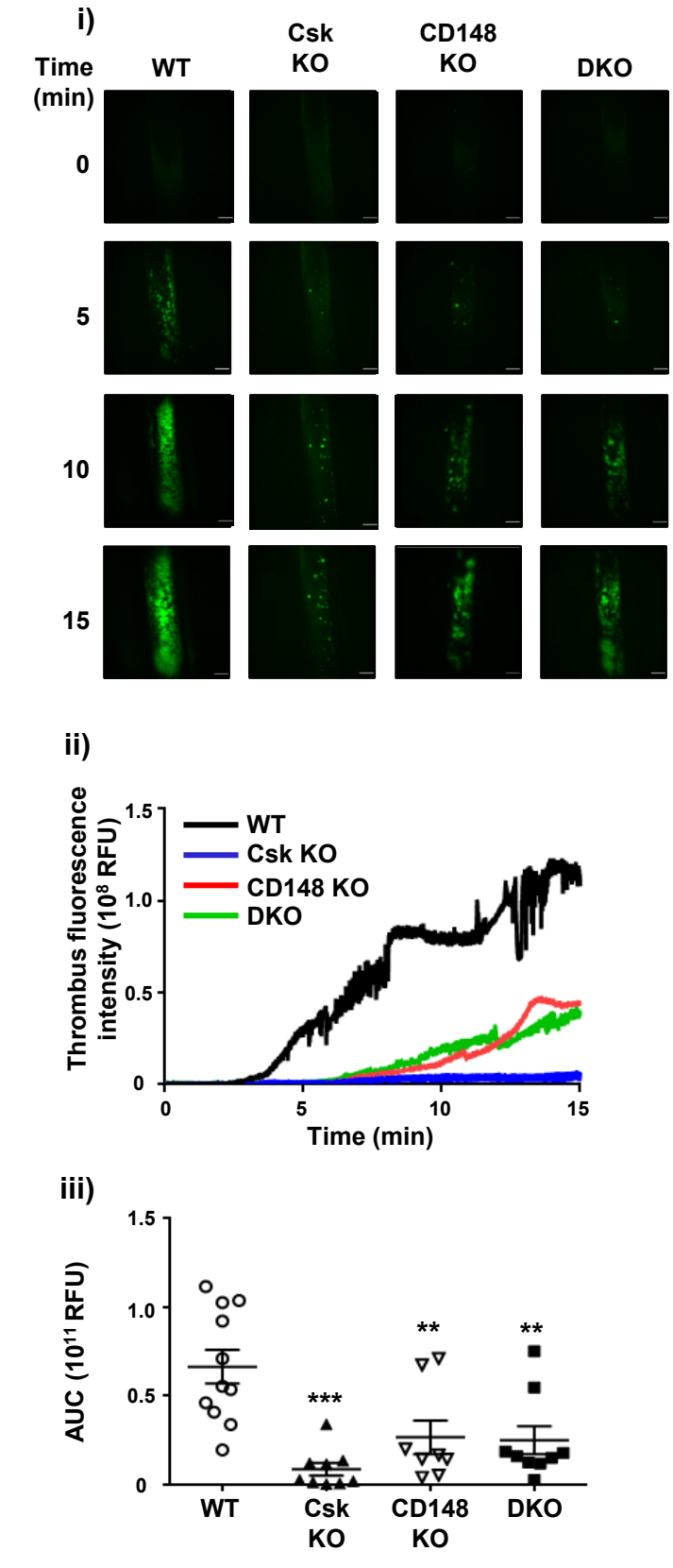
i)
Time (min)
WT
Csk KO
CD148 KO
DKO
0
5
10
15
ii)
Thrombus fluorescence intensity (10^8 RFU)
1.5
1.0
0.5
0
WT
Csk KO
CD148 KO
DKO
0
5
10
15
Time (min)
iii)
AUC (10^{11} RFU)
1.5
1.0
0.5
0
***
**
**
WT
Csk KO
CD148 KO
DKO

Figure 3

A i) collagen

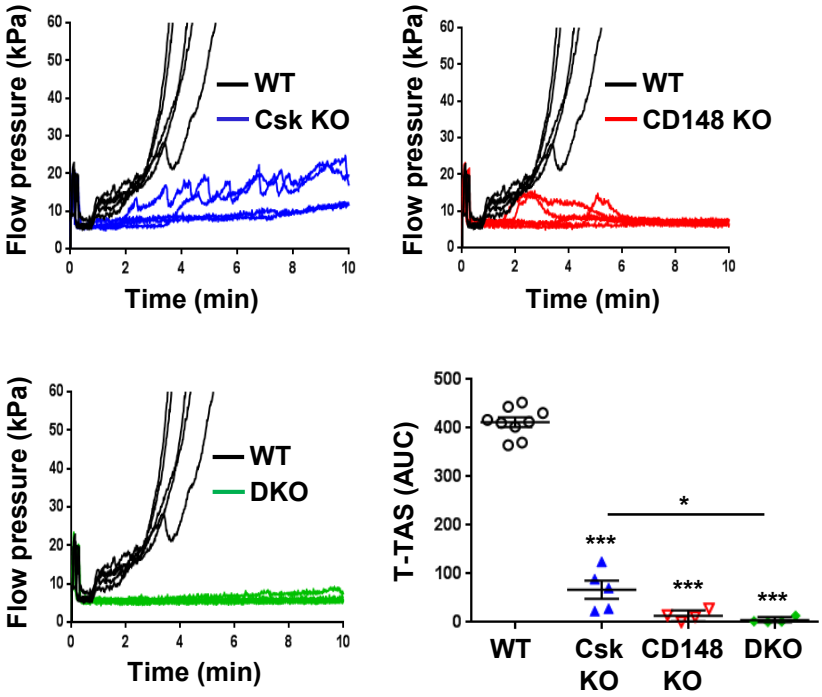

ii) collagen + tissue factor

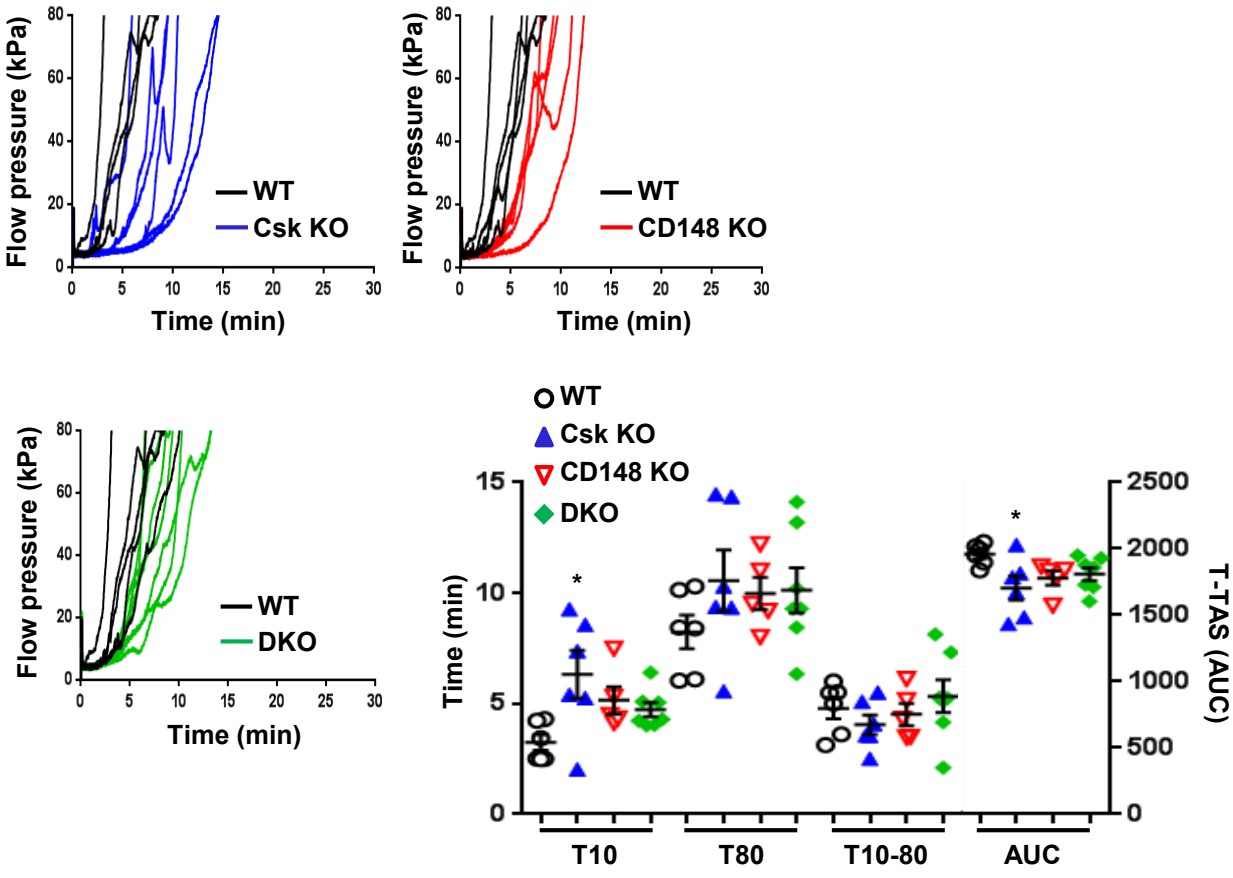

Figure 3

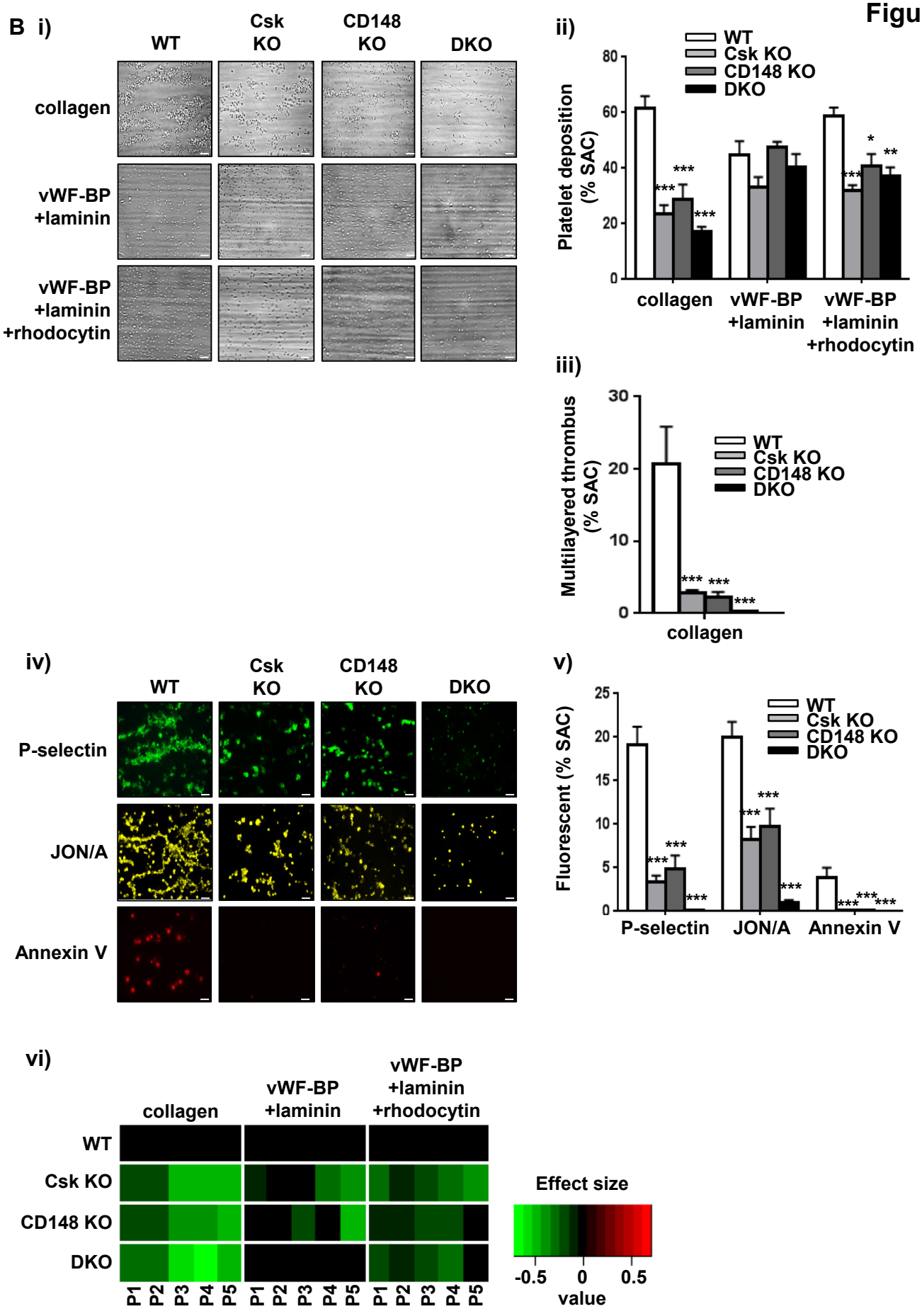
B i)
WT
Csk KO
CD148 KO
DKO
collagen
vWF-BP +laminin
vWF-BP +laminin +rhodocytin
ii)
WT
Csk KO
CD148 KO
DKO
Platelet deposition (% SAC)
collagen
vWF-BP +laminin
vWF-BP +laminin +rhodocytin
iii)
Multilayered thrombus (% SAC)
collagen
iv)
P-selectin
JON/A
Annexin V
v)
Fluorescent (% SAC)
P-selectin
JON/A
Annexin V
vi)
collagen
vWF-BP +laminin
vWF-BP +laminin +rhodocytin
Effect size
-0.5
0
0.5
value
P1 P2 P3 P4 P5

Figure 3

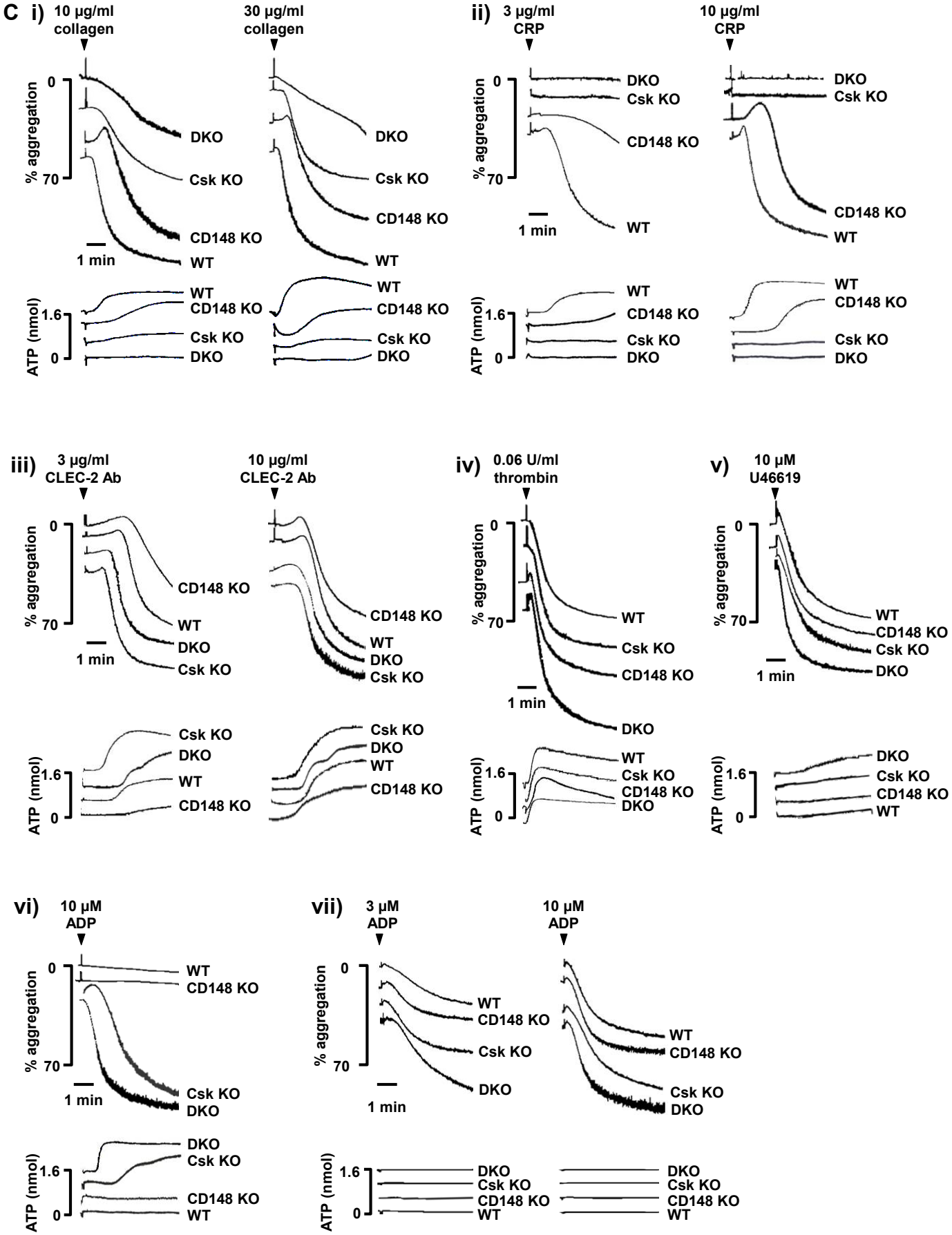
C
i)
10 µg/ml collagen
30 µg/ml collagen
% aggregation
0
70
DKO
Csk KO
CD148 KO
WT
1 min
ATP (nmol)
1.6
0
ii)
3 µg/ml CRP
10 µg/ml CRP
iii)
3 µg/ml CLEC-2 Ab
10 µg/ml CLEC-2 Ab
iv)
0.06 U/ml thrombin
v)
10 µM U46619
vi)
10 µM ADP
vii)
3 µM ADP
10 µM ADP

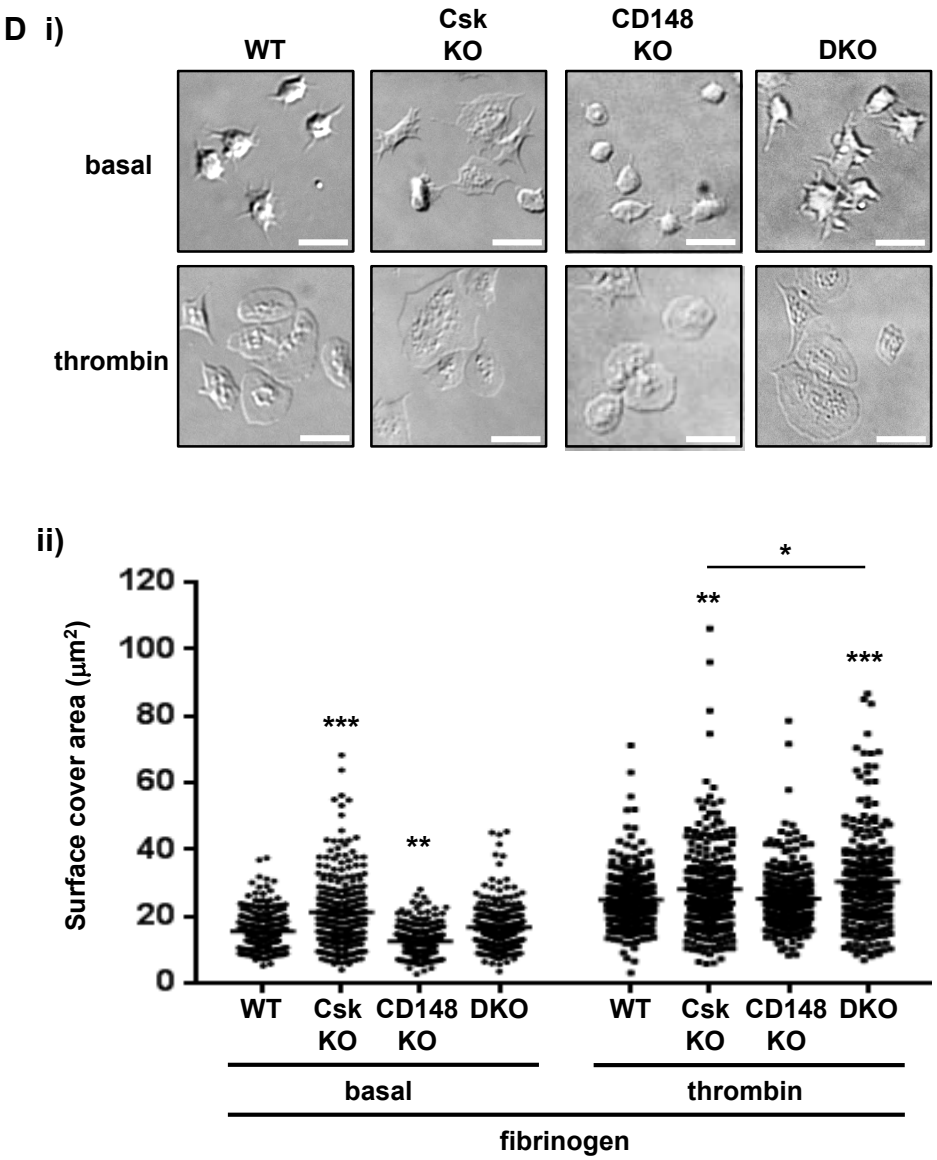
D i)
WT
Csk KO
CD148 KO
DKO
basal
thrombin
ii)
Surface cover area (µm²)
120
100
80
60
40
20
0
***
**
*
**
***
WT
Csk KO
CD148 KO
DKO
WT
Csk KO
CD148 KO
DKO
basal
thrombin
fibrinogen

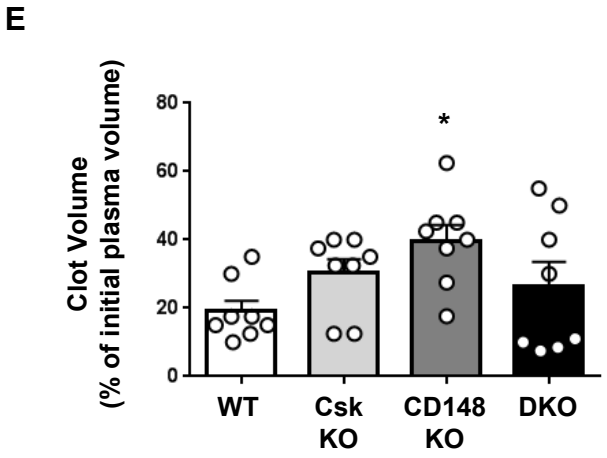
E
Clot Volume (% of initial plasma volume)
80
60
40
20
0
*
WT
Csk KO
CD148 KO
DKO

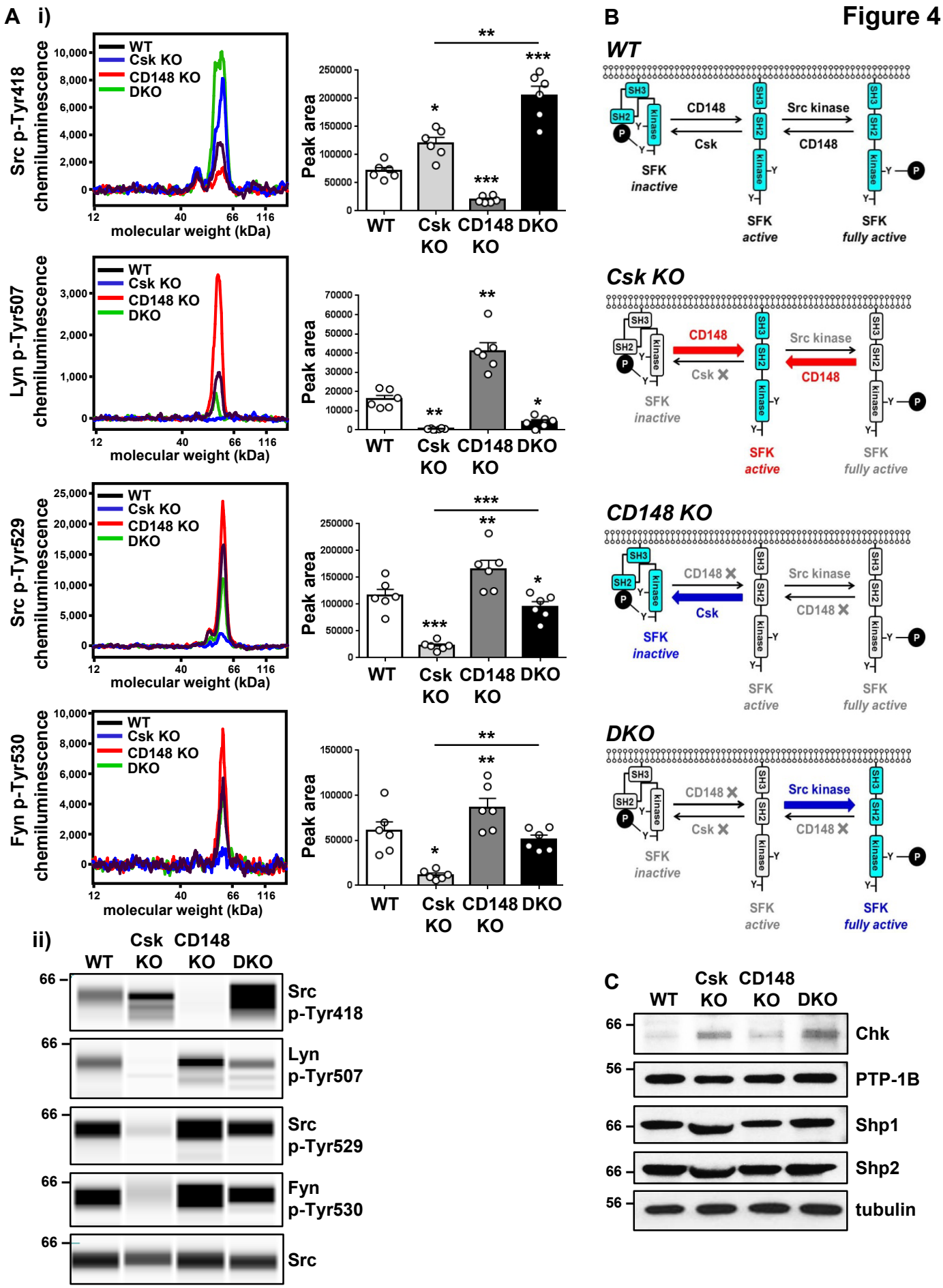
A i)
Src p-Tyr418 chemiluminescence
Lyn p-Tyr507 chemiluminescence
Src p-Tyr529 chemiluminescence
Fyn p-Tyr530 chemiluminescence
WT
Csk KO
CD148 KO
DKO
molecular weight (kDa)
Peak area
WT
Csk KO
CD148 KO
DKO
ii)
Src p-Tyr418
Lyn p-Tyr507
Src p-Tyr529
Fyn p-Tyr530
Src
B
Figure 4
WT
Csk KO
CD148 KO
DKO
SH3
SH2
kinase
SFK inactive
SFK active
SFK fully active
CD148
Csk
Src kinase
C
Chk
PTP-1B
Shp1
Shp2
tubulin

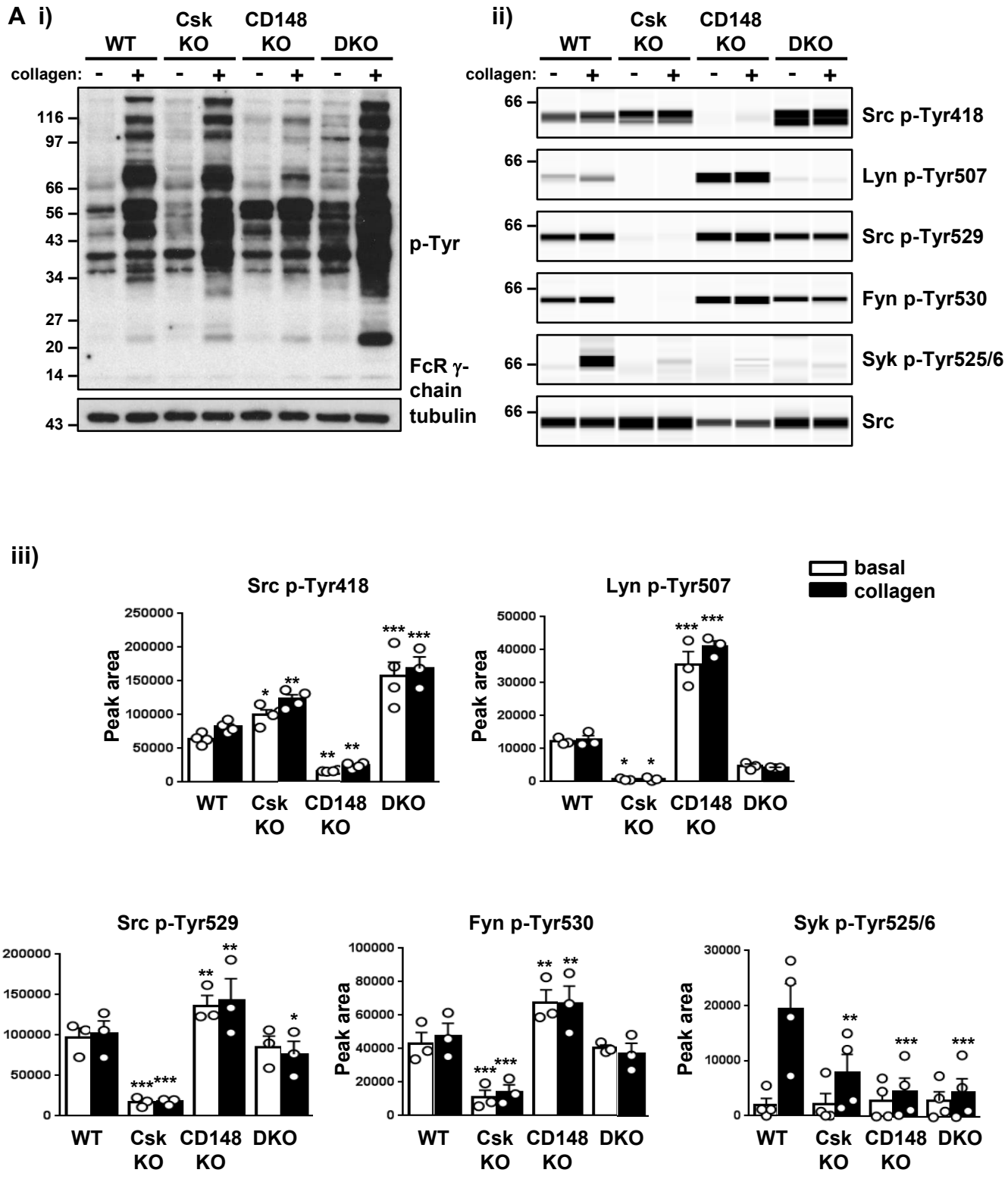
A i)
WT
Csk KO
CD148 KO
DKO
collagen: - + - + - + - +
116
97
66
56
43
34
27
20
14
43
p-Tyr
FcR γ-chain
tubulin
ii)
WT
Csk KO
CD148 KO
DKO
collagen: - + - + - + - +
66
Src p-Tyr418
Lyn p-Tyr507
Src p-Tyr529
Fyn p-Tyr530
Syk p-Tyr525/6
Src
iii)
basal
collagen
Src p-Tyr418
Lyn p-Tyr507
Src p-Tyr529
Fyn p-Tyr530
Syk p-Tyr525/6
Peak area
WT
Csk KO
CD148 KO
DKO

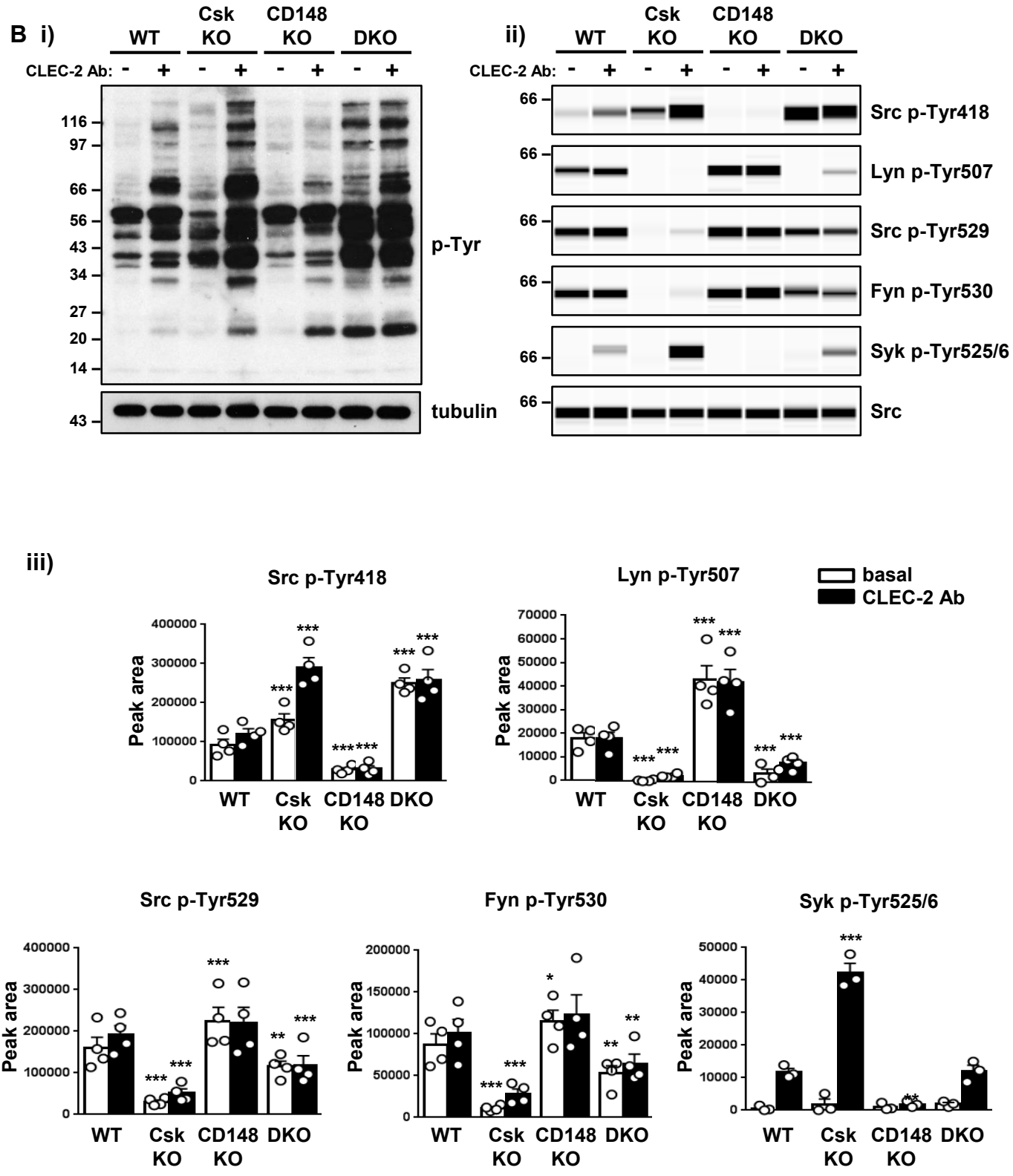
B i)
WT
Csk KO
CD148 KO
DKO
CLEC-2 Ab: - + - + - + - +
116
97
66
56
43
34
27
20
14
p-Tyr
43
tubulin
ii)
WT
Csk KO
CD148 KO
DKO
CLEC-2 Ab: - + - + - + - +
66
Src p-Tyr418
Lyn p-Tyr507
Src p-Tyr529
Fyn p-Tyr530
Syk p-Tyr525/6
Src
iii)
basal
CLEC-2 Ab
Src p-Tyr418
Lyn p-Tyr507
Src p-Tyr529
Fyn p-Tyr530
Syk p-Tyr525/6
Peak area
WT
Csk KO
CD148 KO
DKO

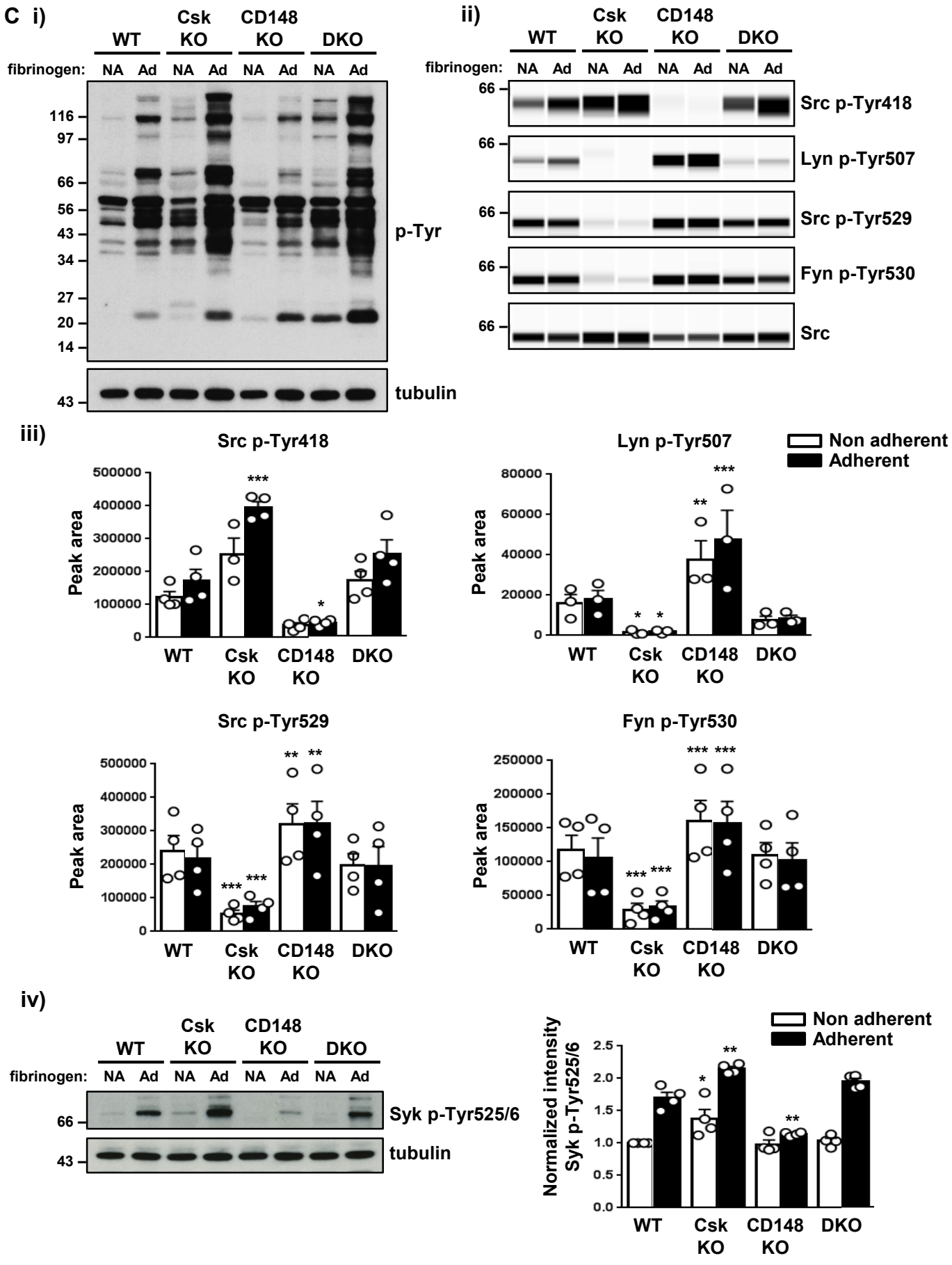
C i)
WT
Csk KO
CD148 KO
DKO
fibrinogen: NA Ad NA Ad NA Ad NA Ad
116
97
66
56
43
34
27
20
14
p-Tyr
43
tubulin
ii)
WT
Csk KO
CD148 KO
DKO
fibrinogen: NA Ad NA Ad NA Ad NA Ad
66
Src p-Tyr418
Lyn p-Tyr507
Src p-Tyr529
Fyn p-Tyr530
Src
iii)
Src p-Tyr418
Lyn p-Tyr507
Non adherent
Adherent
Peak area
WT
Csk KO
CD148 KO
DKO
Src p-Tyr529
Fyn p-Tyr530
iv)
Syk p-Tyr525/6
tubulin
Normalized intensity Syk p-Tyr525/6

D i)

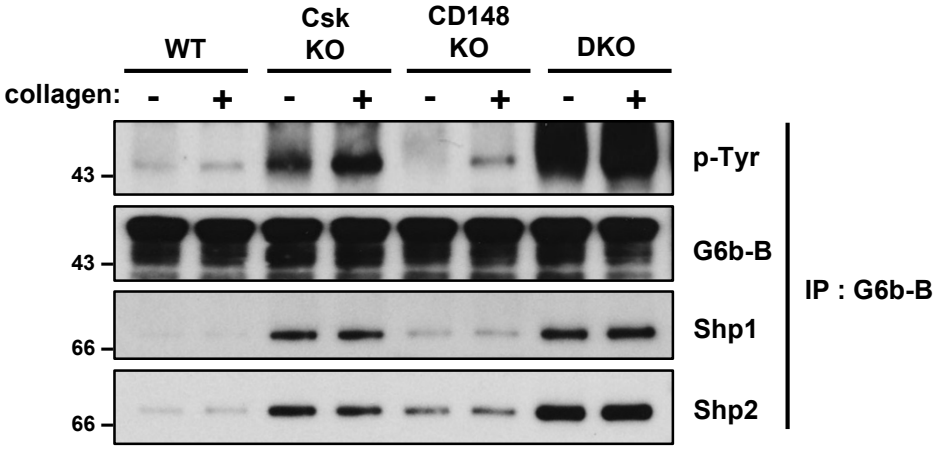
WT
Csk KO
CD148 KO
DKO
collagen: - + - + - + - +
43
43
66
66
p-Tyr
G6b-B
Shp1
Shp2
IP : G6b-B

ii)

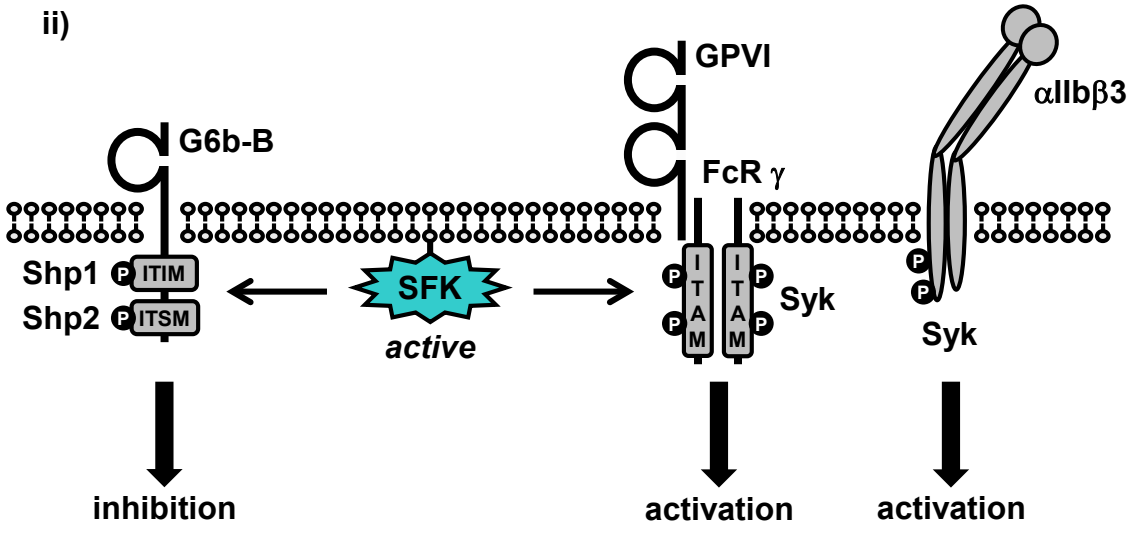
G6b-B
GPVI
FcR γ
αIIbβ3
Shp1
Shp2
ITIM
ITSM
SFK
active
ITAM
ITAM
Syk
Syk
inhibition
activation
activation

Figure 6

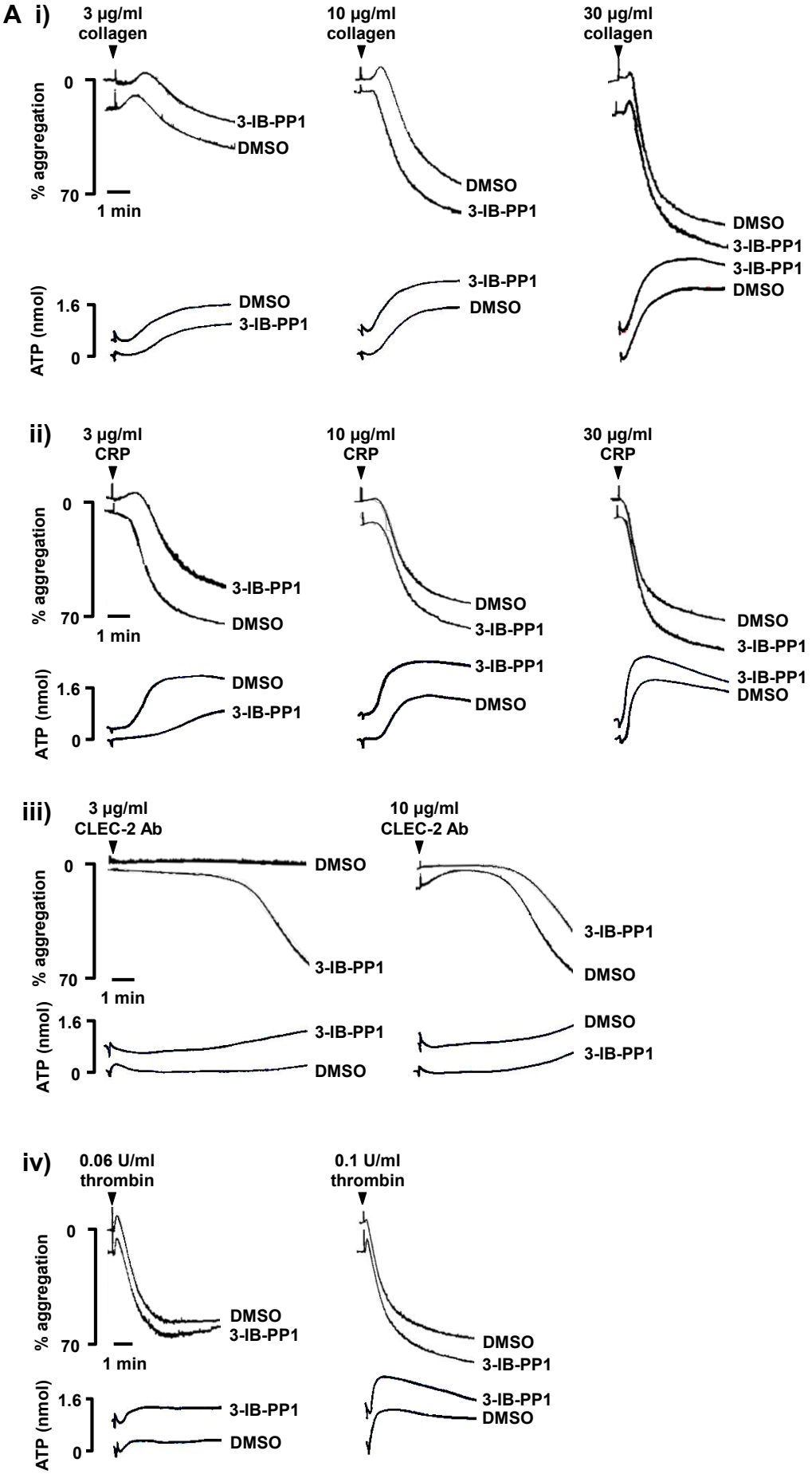
A i)
3 µg/ml collagen
10 µg/ml collagen
30 µg/ml collagen
% aggregation
0
70
1 min
3-IB-PP1
DMSO
ATP (nmol)
1.6
0
ii)
3 µg/ml CRP
10 µg/ml CRP
30 µg/ml CRP
iii)
3 µg/ml CLEC-2 Ab
10 µg/ml CLEC-2 Ab
iv)
0.06 U/ml thrombin
0.1 U/ml thrombin

B i)

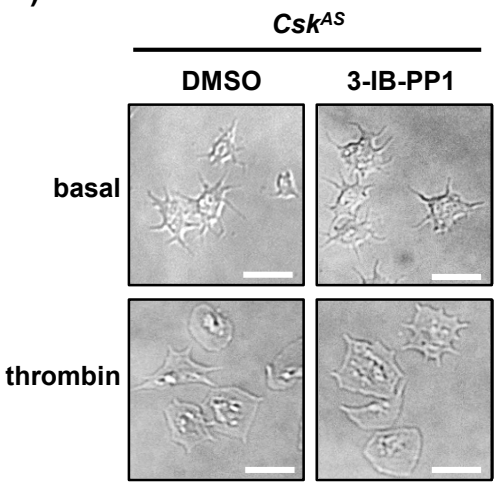
Csk^AS
DMSO
3-IB-PP1
basal
thrombin

ii)

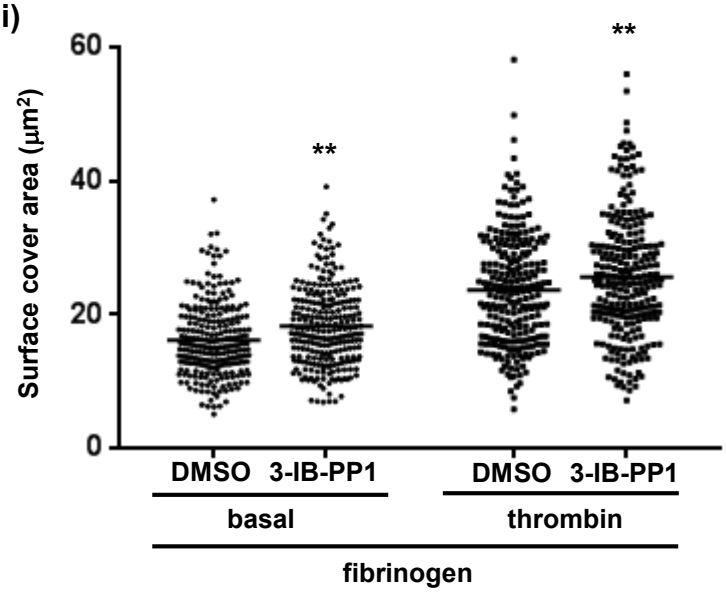
Surface cover area (μm²)
60
40
20
0
**
**
DMSO
3-IB-PP1
DMSO
3-IB-PP1
basal
thrombin
fibrinogen

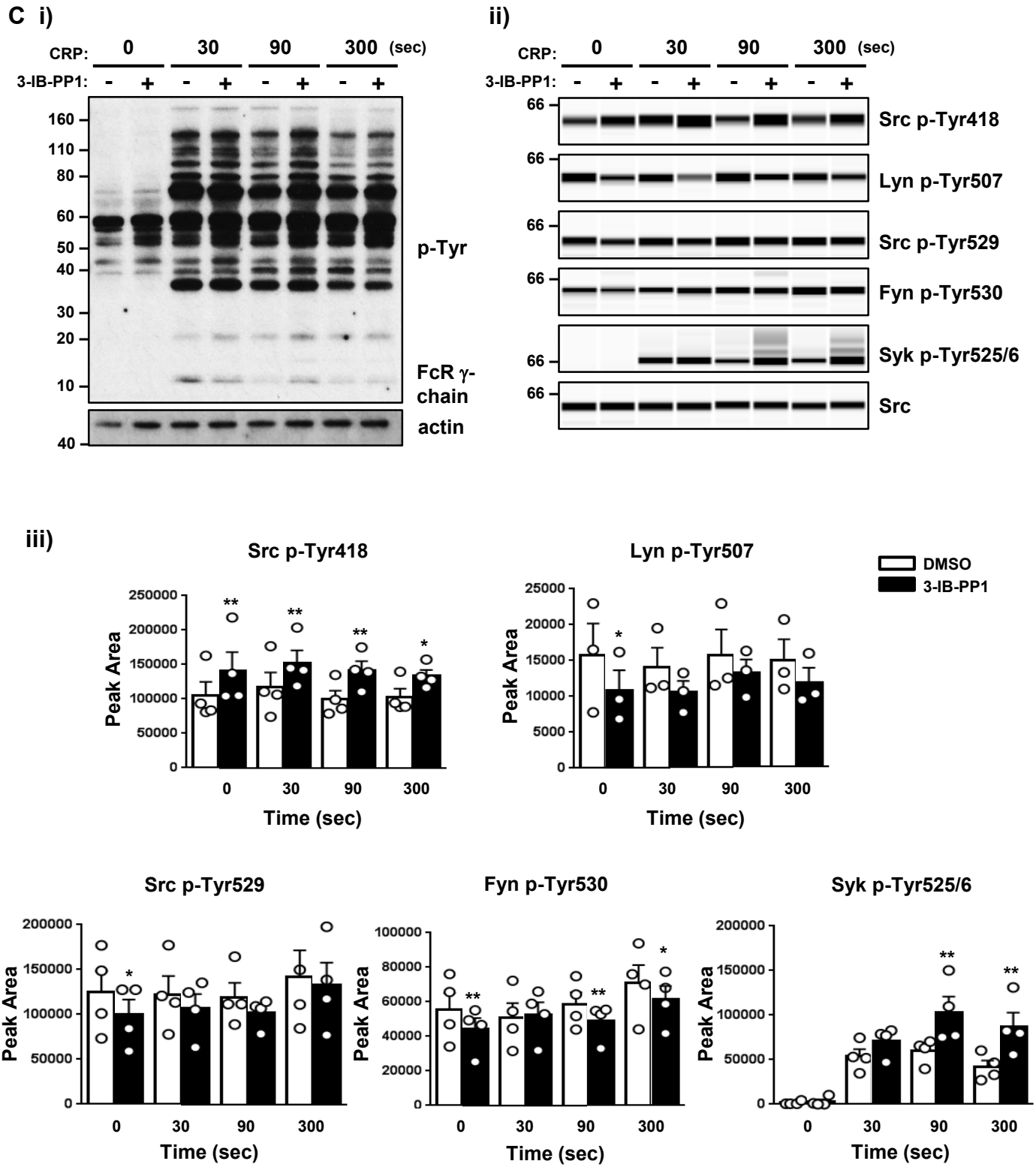
C i)
CRP: 0 30 90 300 (sec)
3-IB-PP1: - + - + - + - +
160
110
80
60
50
40
30
20
10
40
p-Tyr
FcR γ-chain
actin
ii)
CRP: 0 30 90 300 (sec)
3-IB-PP1: - + - + - + - +
66
Src p-Tyr418
Lyn p-Tyr507
Src p-Tyr529
Fyn p-Tyr530
Syk p-Tyr525/6
Src
iii)
Src p-Tyr418
Lyn p-Tyr507
DMSO
3-IB-PP1
Peak Area
Time (sec)
Src p-Tyr529
Fyn p-Tyr530
Syk p-Tyr525/6

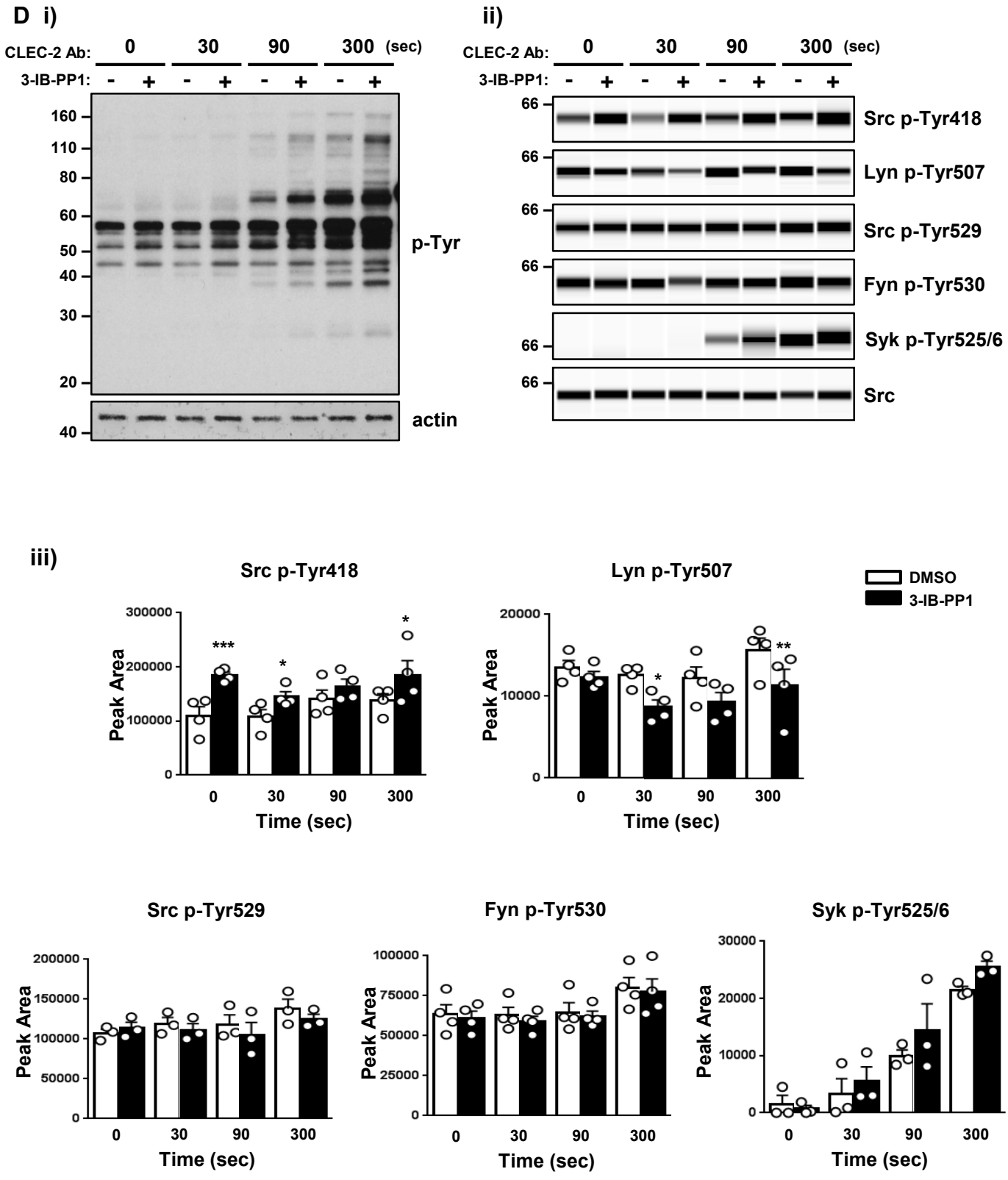
D i)
CLEC-2 Ab: 0 30 90 300 (sec)
3-IB-PP1: - + - + - + - +
160
110
80
60
50
40
30
20
40
p-Tyr
actin
ii)
CLEC-2 Ab: 0 30 90 300 (sec)
3-IB-PP1: - + - + - + - +
66
Src p-Tyr418
Lyn p-Tyr507
Src p-Tyr529
Fyn p-Tyr530
Syk p-Tyr525/6
Src
iii)
Src p-Tyr418
Lyn p-Tyr507
DMSO
3-IB-PP1
Peak Area
Time (sec)
Src p-Tyr529
Fyn p-Tyr530
Syk p-Tyr525/6

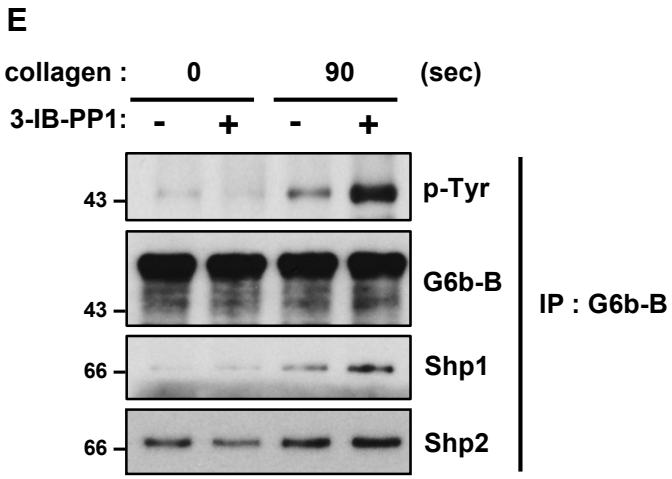
E
collagen :
0
90
(sec)
3-IB-PP1:
-
+
-
+
43
p-Tyr
43
G6b-B
66
Shp1
66
Shp2
IP : G6b-B

Figure 7

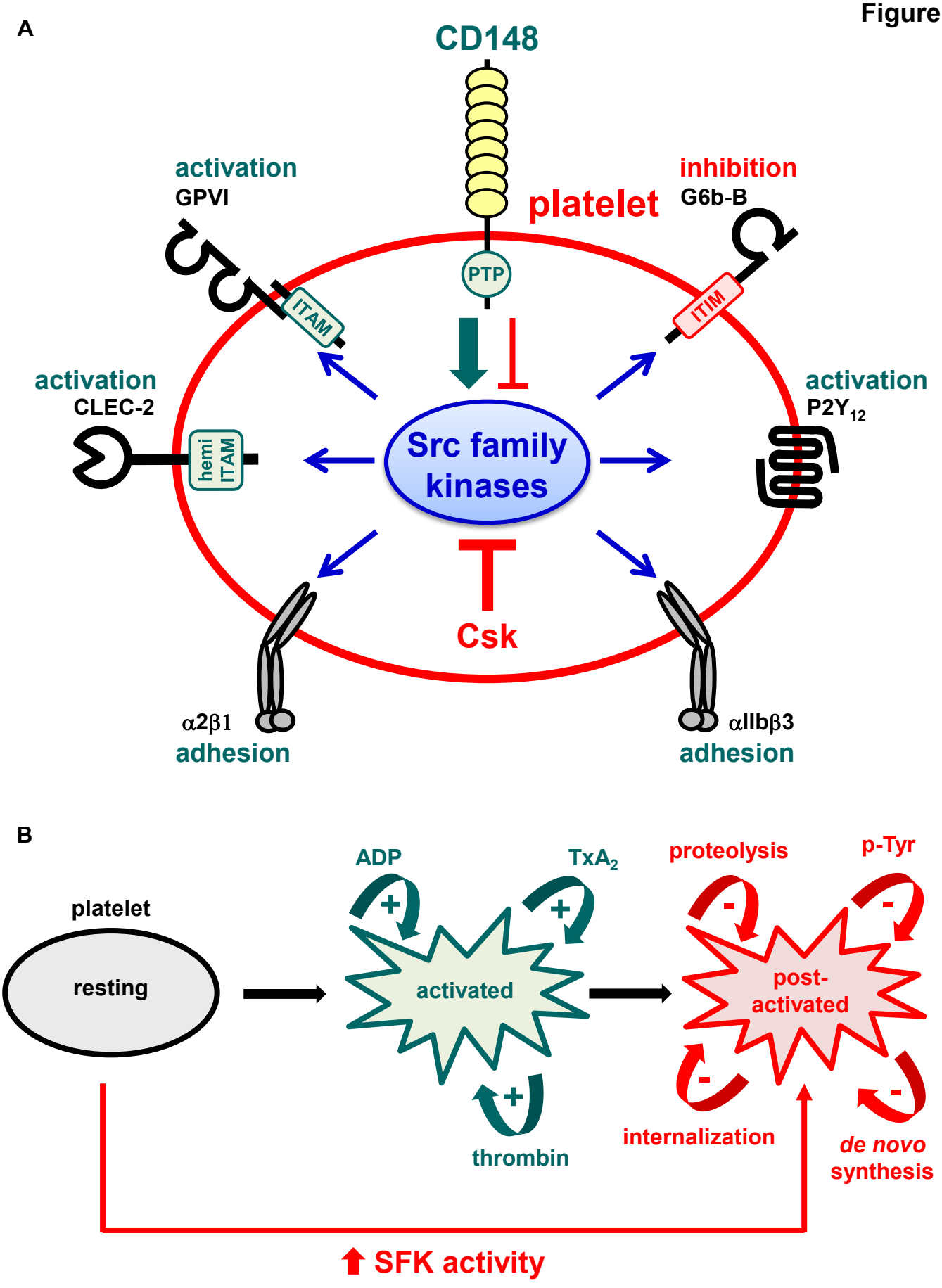
A
CD148
activation
GPVI
platelet
inhibition
G6b-B
PTP
ITAM
ITIM
activation
CLEC-2
hemi ITAM
Src family kinases
activation
P2Y12
Csk
α2β1
adhesion
αIIbβ3
adhesion
B
platelet
resting
ADP
TxA2
activated
thrombin
proteolysis
p-Tyr
post-activated
internalization
de novo synthesis
SFK activity

Supplemental Materials and Methods

Antibodies

The following antibodies were used in this study: anti-GPIbα (Xia.G5), anti-Integrin α2 (Sam.G4), anti-GPVI (JAQ1), anti-P-selectin (Wug.E9), anti-high affinity conformation of CD41/CD61 (JON/A), rat IgG, anti-GPIbα for platelet depletion (R300), and anti-GPIbβ for in vivo mouse platelet labelling (X488) from emfret ANALYTICS; anti-CD41 (MWReg30) and Streptavidin from BD Pharmingen; anti-ADAM10 ectodomain (139712) from R&D system; anti-CLEC-2 (17D9) and rat IgG2b from AbD Serotec; anti-Csk (C-20), anti-Ctk (Chk, C-20), anti-SH-PTP1 (C-19), anti-SH-PTP2 and anti-rat IgG-HRP from Santa Cruz; anti-Src (pY418), anti-Src (pY529), annexin V Alexa Fluor 647 conjugate, and Alexa Fluor 488 and Alexa Fluor 647 antibody labelling kit from Invitrogen Life Technologies; anti-Lyn (pY507), anti-Syk (pY525/526), anti-Syk (D1I5Q) and anti-Src from Cell Signaling; anti-Fyn (pY530) and anti-syrian hamster IgG-HRP from Abcam; anti-PTP-1B, anti-Fc epsilon RI gamma subunit, and anti-phophotyrosine (4G10) from Millipore; anti-α-tubulin (DM1A) from Sigma; anti-mouse and anti-rabbit ECL HRP conjugates from GE Healthcare; anti-CD148 (8A-1) antibody has been previously described;[1] anti-G6b-B (68-3), (N24) and anti-GPVI antibodies have been previously described.[2] Anti-fibrin antibody (clone 59D8), a generous gift from Dr. Timothy J. Stalker (University of Pennsylvania), has been previously described,[3] and labeled using Alexa Fluor monoclonal antibody labeling kits from Invitrogen.

Platelet clearance

Mice were injected intravenously with 150 μl of biotin-*N*-hydroxysuccinamide (4 mg/ml in saline, Sigma-Aldrich). The percentage of biotin$^+$αIIb$^+$ platelets in blood was measured in αIIb$^+$ cells co-stained with streptavidin daily post-injection and the percentage of labelled platelets remaining in the circulation was determined by flow cytometry. The rate of platelet

clearance was determined by a proportionate slope from linear trend lines between days 1 to 3.

Immunohistochemistry

Spleens and femurs were fixed in buffered formalin and embedded in paraffin. Sections (5 μm) were hematoxylin and eosin (H&E) or reticulin stained. Images were obtained by Slide Scanner Axio Scan.Z1 brightfield microscope and Axio Zen software (Zeiss). Analysis of MK counts in spleen and femur per view was performed in a double blinded manner.

Isolation of bone marrow cells and *in vitro* differentiation of megakaryocytes

Bone marrow was flushed using DMEM media supplemented with 10 % FBS, glutamine and penicillin/streptomycin using a 25 gauge needle from femora and tibiae of mice and the cells were spun down. Bone marrow cells were resuspended in ACK buffer (0.15 M NH_4Cl, 1 mM $KHCO_3$, 0.1 mM Na_2EDTA, pH 7.3) in order to lyse erythrocytes and filtered by a 70 μm nylon mesh and subsequently resuspended in P2 buffer (PBS, 5 % FBS, 1 % BSA) for flow cytometry assay. Surface protein expression was measured in bone marrow cells with indicated FITC- or PE-conjugated antibodies by flow cytometry (BD FACSCalibur). Median fluorescence intensity (MFI) were measured in αIIb^+ gated population, and analysed at least 50,000 events for bone marrow cells. To culture megakaryocytes (MKs) for biochemical assay, cells expressing one or more of the lineage specific markers on their surface ($CD16/CD32^+$, $Gr1^+$, $B220^+$, $CD11b^+$) were depleted using immunomagnetic beads (sheep anti-rat IgG Dynabeads). The remaining population was cultured in 2.6% serum-supplemented Stempro medium with 2 mM L-glutamine, penicillin/streptomycin and 20 ng/ml murine SCF at 37°C and 5% CO_2 for 2 days. Cells were then cultured for a further 4 days in the presence of 20 ng/ml SCF and 50 ng/ml Tpo. After 4 days of culture in the

presence of Tpo, mature MKs were enriched using a 1.5%/3% BSA gradient under gravity (1 ×*g*) for 45 minutes at room temperature. MKs were starved for 3 hrs at 37°C in serum-free media to obtain whole-cell lysates as previously described.[4]

Total thrombus-formation analysis system (T-TAS)

Blood treated with 25 μg/ml hirudin was perfused with collagen-coated chip with shear rate 1000 s^{-1} for 10 minutes. Blood treated with 3.2% sodium citrate, 12 mM $CaCl_2$ and 50 μg/ml corn trypsin inhibitor was perfused with collagen plus tissue thromboplastin (tissue factor)-coated chip with shear rate 240 s^{-1} for 30 minutes. Individual time-dependent flow pressure curves, time to onset (T10), time to occlusion (T80), rate of thrombus growth (T10-80) and total thrombogenicity (Area under the curve: AUC) were measured by the total thrombus-formation analysis system (T-TAS, Fujimori Kogyo, Japan).

Whole-blood thrombus formation and platelet adhesion under flow

Mouse blood anticoagulated with 5 Unit/ml heparin, 40 μM PPACK and 50 Unit/ml fragmin was perfused for 3.5 minutes at 1,000 s^{-1} over glass coverslips coated with microspots of agonists; 100 μg/ml collagen type I, 12.5 μg/ml vWF-binding peptide (VWF-BP), 50 μg/ml laminin, and 250 μg/ml rhodocytin. Brigtfield and three-color fluorescence images were captured with an EVOS microscope (60x oil) (Life Technologies) and analysed using Fiji as previously described.[5]

Platelet aggregation and secretion

Aggregation and adenosine triphosphate (ATP) secretion were performed in a lumi-aggregometer (Chrono-Log, Havertown, PA) with continuous stirring at 1200 rpm at 37 °C for the times shown, and monitored by measuring changes in light transmission.

Static adhesion spreading assay

Washed platelets were pre-incubated with or without thrombin (0.1 Unit/ml, 5 minutes) placed on fibrinogen-coated cover-slips (100 μg/ml, 45 minutes, 37°C) and imaged (63x oil immersion lens), as previously described.[6]

Clot retraction

Platelet-rich plasma (PRP) was prepared from blood treated with 4% (w/v) sodium citrate by centrifugation at 200 g for 8 minutes at room temperature in the presence of prostacyclin (0.1 μg/ml) and adjusted to a concentration of 2 x 10^8 platelets/ml by platelet-poor plasma (PPP) which was prepared by centrifugation 1000 g for 10 minutes at room temperature. Fibrin clot retraction was performed by incubating 200 μl of PRP (4 x 10^7 platelets) in the presence of 1 Unit/ml thrombin and 2 mM $CaCl_2$ for 2 hours at room temperature in an aggregometer cuvette. A paper clip was added to facilitate clot removal at the termination of the experiment. The volume of residual clot-free plasma was determined, and clot volume was taken as 200 μl minus this value. Clot volume was expressed as a percentage of the original 200 μl plasma volume.

Platelet stimulation for biochemical analysis

For biochemical analysis of GPVI and CLEC-2 signaling pathways, platelets were pre-incubated with lotrafiban (10 μM), apyrase (2 Unit/ml) and indomethacin (10 μM) for 10 minutes. Afterwards, platelets were stimulated under stirring conditions (1200 rpm, 37°C) with collagen, CRP or CLEC-2 antibody for indicated times.

For biochemical analysis of the integrin αIIbβ3 outside-in signaling pathway, platelets were pre-incubated with apyrase (2 Unit/ml) and indomethacin (10 μM) for 10

minutes, and then placed on fibrinogen-coated plates (100 μg/ml) for 45 minutes at 37°C. Non-adherent platelets were used as controls.

After stimulating GPVI, CLEC-2 or αIIbβ3 outside-in signaling pathways for the specified times, platelets were lysed with an equal volume of ice cold 2 x lysis buffer (2% Nonidet P-40, 300 mM NaCl, 20 mM Tris, 10 mM EDTA, 2 mM Na_3VO_4, 200 μg/ml 4-(2-aminoethyl) benzenesulfonyl fluoride hydrochloride, 10 μg/ml leupeptin, 10 μg/ml aprotinin, and 1 μg/ml pepstasin A, pH 7.4). In case of fibrinogen-adherent platelets, ice cold 1 x lysis buffer was used to lyse cells for 15 minutes on ice, which was followed by scraping platelets off the plates. Insoluble cell debris was removed by centrifugation for 5 minutes at 13,000 x g, 4°C, and whole cell lysates (WCLs) were precleared using protein G- or A-Sepharose (Sigma-Aldrich) for 30 minutes. G6b-B was immunoprecipitated from collagen-stimulated WCLs with anti-G6b-B antibody as previously described.[2]

Immunoblotting

WCLs were either boiled in SDS-loading buffer, and analyzed by SDS-PAGE and traditional Western blotting or analyzed on an automated capillary-based immunoassay platform; Wes (ProteinSimple, San Diego, USA) for quantitative analysis. WCLs to be analyzed on the Wes system were prepared according to manufacturer's instructions and were not precleared. Protein concentrations were determined using the Bio-Rad RC DC protein assay. Diluted samples and primary antibody were added to pre-filled microplates with Split Running Buffer (PS-MK14). Before analyzing WCLs from transgenic mouse platelets, optimal lysate and antibody concentrations were determined on *WT* WCLs. Briefly, for each antibody used, a lysate dilution experiment was performed to confirm the optimal dynamic range of the protein on Wes. This was followed by an antibody optimization experiment to compare a range of dilutions and select an antibody concentration near to saturation level to allow a

quantitative comparison of signals between samples. In each run, twenty-four samples were analyzed in parallel as triplicates of eight samples from the same experiment for either Src, Src p-Tyr418 and Lyn p-Tyr507 on one microplate (plate A) or Src p-Tyr529, Fyn p-Tyr530 and Syk p-Tyr525/6 on another microplate (plate B). Compass Software (ProteinSimple, San Diego, USA) was used to operate Wes and analyze results. Separation time was set to 31 minutes, stacking loading time to 21 seconds and sample loading time to 9 seconds for both microplates. Primary antibody incubation time was 60 minutes for plate A and 30 minutes for plate B, and exposure times were 5; 15; 30; 60; 120; 240 and 480 seconds for plate A and 2; 5; 10; 20; 40; 80 and 160 seconds for plate B. The defined antibody and lysate concentrations were as follows: anti-Src antibody (1:50 dilution), anti-Src p-Tyr529 antibody (1:100 dilution) and anti-Fyn p-Tyr530 antibody (1:50 dilution) were used for 0.025 mg/ml platelet and 0.1 mg/ml MK lysate concentration; anti-Src p-Tyr418 antibody (1:10 dilution) was used for 0.05 mg/ml platelet and 0.1 mg/ml MK lysate concentration; anti-Lyn p-Tyr507 antibody (1:10 dilution) was used for 0.2 mg/ml platelet and 0.4 mg/ml MK lysate concentration; anti-Syk p-Tyr525/6 antibody (1:50 dilution) was used for 0.1 mg/ml platelet lysate concentration. The only exception from the above described concentrations were CLEC-2-stimulated samples in Figure 6 B in which case Syk p-Tyr525/6 antibody (1:50 dilution) was used in combination with 0.05 mg/ml platelet lysate concentrations.

Statistical analysis

Quantification of data is indicated in the figures, figure legends and methods sections. Statistical parameters including the exact value of n, the definition of center, dispersion and precision measures (mean ± SEM) and statistical significance are reported in the figures and figure legends. Sample number (n) indicates the number of independent biological replicates in each experiment in most figures, the number of images of H&E-stained spleen and femur

sections in Figure S6A-B, the number of individual platelets in Figure 3Dii and 6Bii, and the number of injury induced in Figure 2Ciii. For multiple group comparisons, one-way or two-way ANOVA followed by *post-hoc* tests was used to determine statistical significance. Data from the Wes system were analyzed using repeated measures (RM) one-way ANOVA (Figure 4Ai and Figure S8A) or RM two-way ANOVA (Figures 5A-C and 6C-D) to control for variability in different experiments and Wes runs or by t-test (Figure S9D). RM two-way ANOVA was also used to analyze data from traditional Western blots (Figure 5Civ). Ordinary one- or two-way ANOVA was used to analyze the rest of the figures. P values < 0.05 were considered significant. In figures, asterisks denote statistical significance compared to *WT* (Figure 1-5) or DMSO-incubated control samples (Figure 6). Statistical analysis was performed in GraphPad Prism 6 (GraphPad Software, La Jolla, CA), except statistical analysis of platelet clearance and recovery, which were performed in Excel.

References

1. Lin J, Weiss A. The tyrosine phosphatase CD148 is excluded from the immunologic synapse and down-regulates prolonged T cell signaling. *J Cell Biol*. 2003;162(4):673-682.

2. Mazharian A, Wang YJ, Mori J, et al. Mice lacking the ITIM-containing receptor G6b-B exhibit macrothrombocytopenia and aberrant platelet function. *Sci Signal*. 2012;5(248):ra78.

3. Stalker TJ, Traxler EA, Wu J, et al. Hierarchical organization in the hemostatic response and its relationship to the platelet-signaling network. *Blood*. 2013;121(10):1875-1885.

4. Smith CW, Thomas SG, Raslan Z, et al. Mice Lacking the Inhibitory Collagen Receptor LAIR-1 Exhibit a Mild Thrombocytosis and Hyperactive Platelets. *Arterioscler Thromb Vasc Biol*. 2017;37(5):823-835.

5. de Witt SM, Swieringa F, Cavill R, et al. Identification of platelet function defects by multi-parameter assessment of thrombus formation. *Nat Commun*. 2014;5:4257.

6. Senis YA, Tomlinson MG, Ellison S, et al. The tyrosine phosphatase CD148 is an essential positive regulator of platelet activation and thrombosis. *Blood*. 2009;113(20):4942-4954.

Table S1. Hematological analysis of *Csk KO, CD148 KO* and *DKO* mice.

Parameter	***WT*** (n = 42-67)	***Csk KO*** (n = 26)	***CD148 KO*** (n = 12 -18)	***DKO*** (n = 24-27)
PLT ($10^3/\mu L$)	825.1 ±83.1	289.9 ±125.15***	772.0 ±96.2	809.3 ±197.5
MPV (fL)	5.65 ±0.38	7.14 ±1.36***	5.78 ±0.46	6.60 ±0.53***
RBC ($10^6/\mu L$)	9.68 ± 1.07	9.03 ± 0.67	9.63 ± 1.40	9.37 ± 0.86
HCT (%)	28.07 ± 3.94	27.29 ± 2.07	26.31 ± 5.02	27.36 ± 2.64
WBC ($10^3/\mu L$)	7.39 ± 2.86	8.40 ± 3.80	8.37 ± 4.32	11.61 ± 4.98***
LYM ($10^3/\mu L$)	6.56 ± 2.53	6.91 ± 3.36	7.02 ± 3.78	8.84 ± 4.09*
MON ($10^3/\mu L$)	0.28 ± 0.24	0.67 ± 0.40***	0.48 ± 0.49	1.58 ± 0.70***
NEU ($10^3/\mu L$)	0.53 ± 0.38	0.74 ± 0.33	0.76 ± 0.62	1.05 ± 0.44***
EOS ($10^3/\mu L$)	0.008 ± 0.03	0.01 ± 0.03	0.02 ± 0.05	0.04 ± 0.07*
BAS ($10^3/\mu L$)	0.03 ± 0.06	0.07 ± 0.07	0.03 ± 0.04	0.10 ± 0.19*

PLT, platelets; MPV, mean platelet volume; RBC, red blood cells; HCT, haematocrit, WBC, white blood cells; LYM, lymphocytes; MON, monocytes; NEU, neutrophils; EOS, eosinophils; BAS, basophils
Mean ± standard deviation, *$P < 0.05$, ***$P < 0.001$, one-way ANOVA with Tukey's test

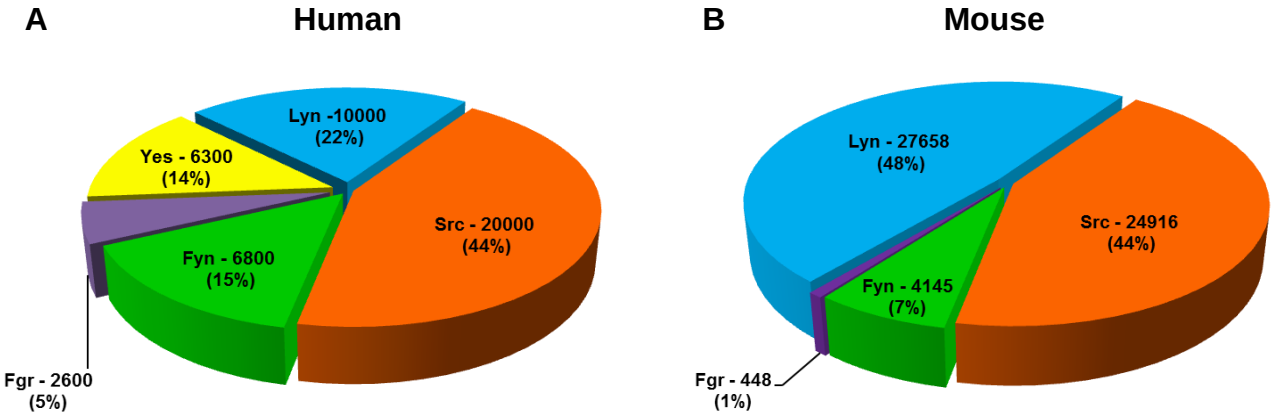

Figure S1. Expression levels of SFKs in platelets.
Number of copies of SFKs' expression in (A) human platelets[3] and (B) mouse platelets[4] are displayed as percentage values in a pie chart.

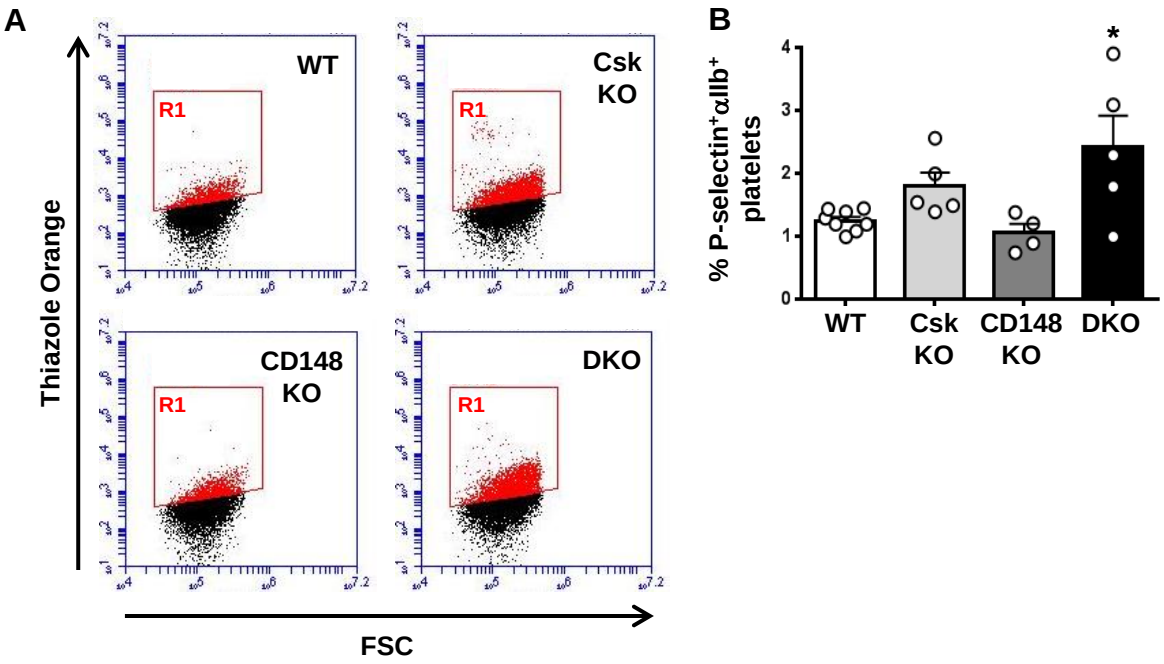

Figure S2. Increased immature platelet fraction but normal platelet P-selectin expression in *Csk KO* mice. (A) Representative image of reticulated platelet population in flow cytometry. Reticulated platelets in whole blood were measured in thiazole orange/αIIb double-positive cells detected by flow cytometry. αIIb positive platelets in whole blood are gated and the percentage of reticulated platelets was determined in region 1 (R1; in red) in dot plot diagram forward scatter (FSC) vs. RNA dye (Thiazole Orange). See also Figure 1C. (B) Percentage of P-selectin$^+$αIIb$^+$ platelets in blood. *P < 0.05, one-way ANOVA with Tukey's test, mean ± SEM.

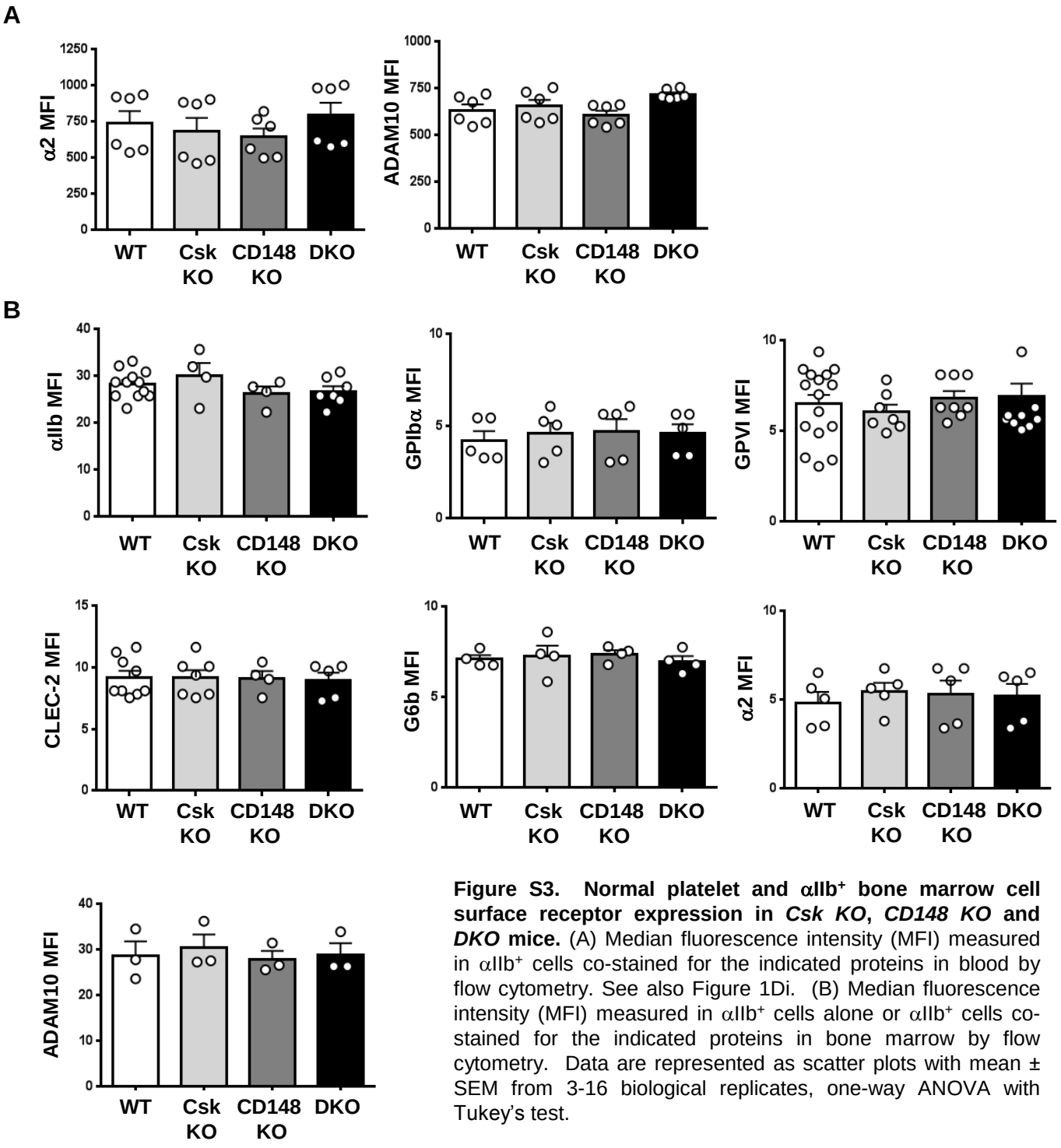

Figure S3. Normal platelet and αIIb⁺ bone marrow cell surface receptor expression in *Csk KO*, *CD148 KO* and *DKO* mice. (A) Median fluorescence intensity (MFI) measured in αIIb⁺ cells co-stained for the indicated proteins in blood by flow cytometry. See also Figure 1Di. (B) Median fluorescence intensity (MFI) measured in αIIb⁺ cells alone or αIIb⁺ cells co-stained for the indicated proteins in bone marrow by flow cytometry. Data are represented as scatter plots with mean ± SEM from 3-16 biological replicates, one-way ANOVA with Tukey's test.

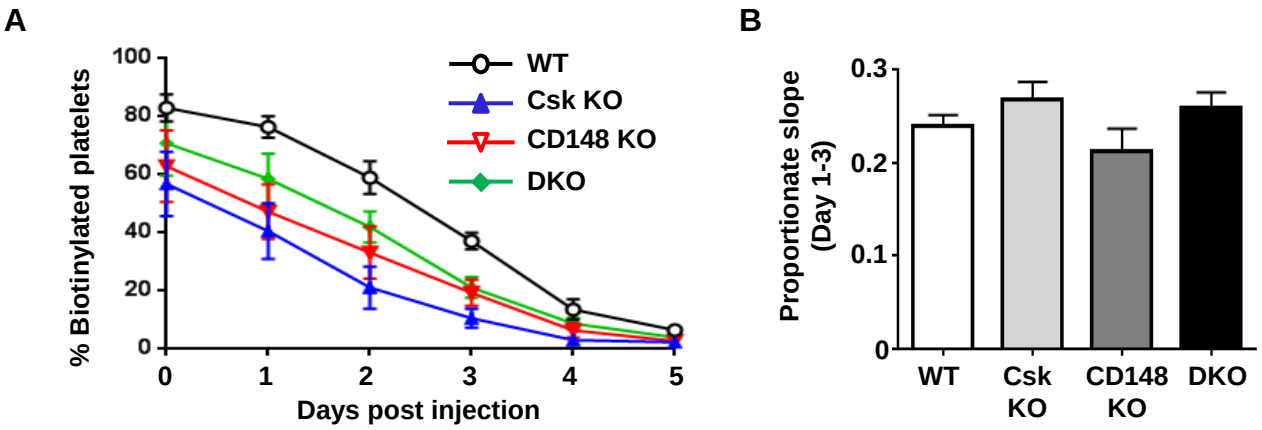

Figure S4. Normal platelet clearance in *Csk KO* mice. (A) Percentage of biotin$^{+}\alpha$IIb^{+} platelets in blood of post-injection of 150 µl biotin-*N*-hydroxysuccinamide. (B) The rate of platelet clearance determined by a proportionate slope from linear trend lines between day 1 to 3 from (A), n = 6 mice/time point/genotype. One-way ANOVA with Dunnett's test; vs *WT*, mean ± SEM.

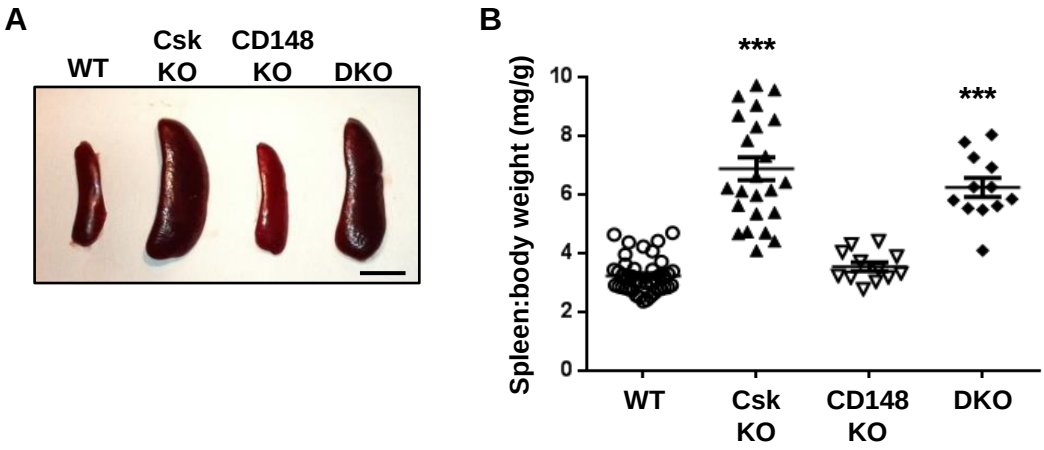

Figure S5. Splenomegaly in *Csk KO* and *DKO* mice. (A) Gross morphology of representative spleens (scale bar: 5 mm) and (B) spleen/body weight ratio.
****P* < 0.001, one-way ANOVA with Tukey's test

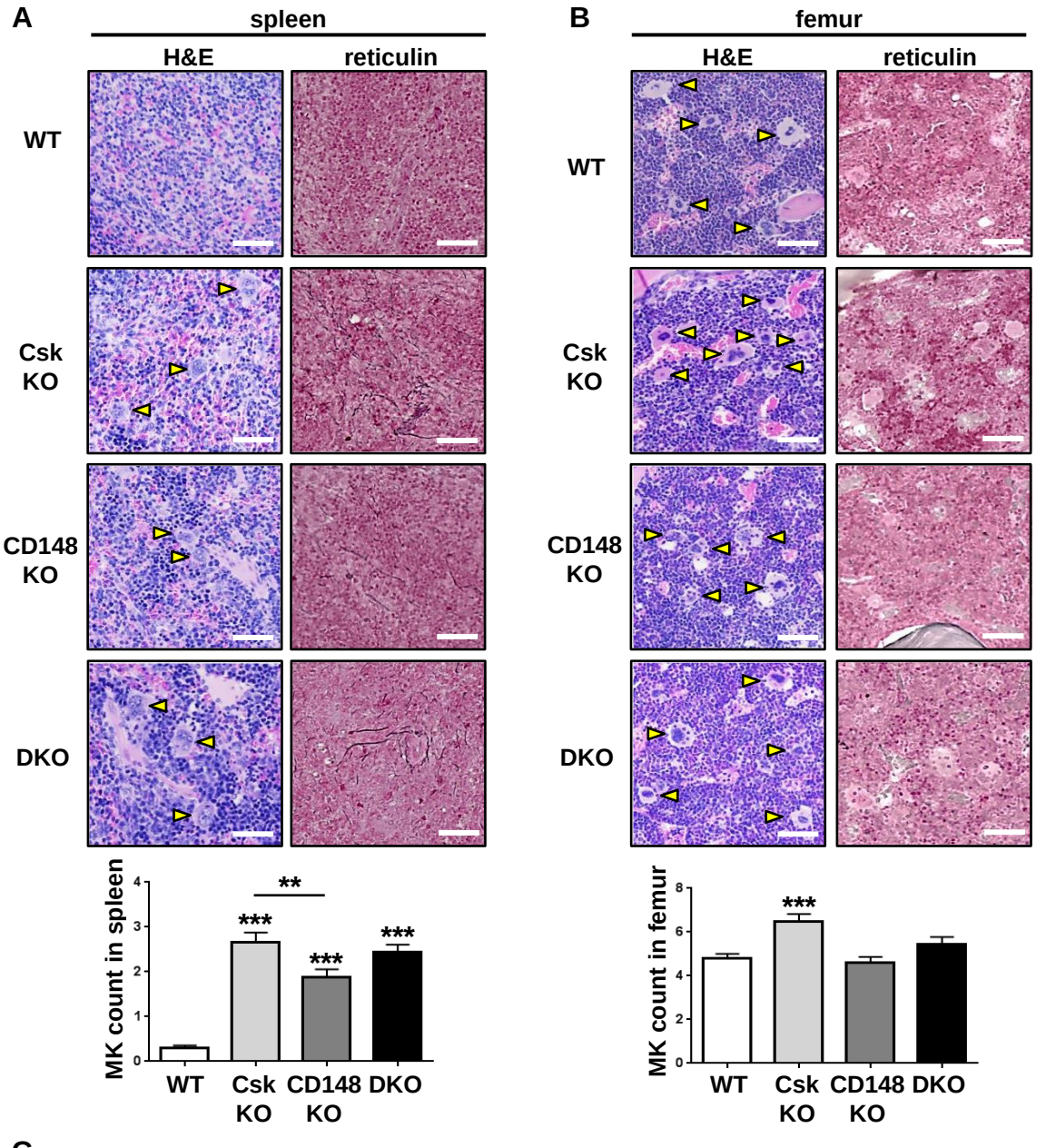

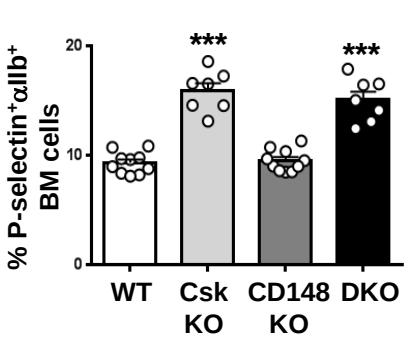

Figure S6. Extramedullary hematopoiesis and myelofibrosis in *Csk KO* and *DKO* mice. (A-B) Representative Haematoxylin and eosin (H&E) and reticulin staining in (A) spleen and (B) femur (scale bar: 50 μm). Analysis of megakaryocyte (MK) count per view was performed in a double-blinded manner., n = 75-100 images from 5 mice/genotype. (C) Percentage of P-selectin$^+\alpha$IIb$^+$ bone marrow (BM) cells. $^{**}P < 0.05$, $^{***}P < 0.001$, one-way ANOVA with Tukey's test , mean ± SEM.

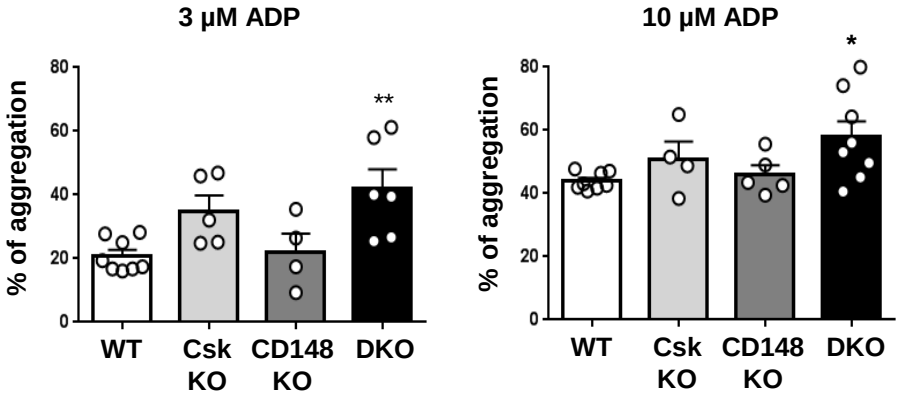

Figure S7. Increased ADP response in *DKO* mice. ADP-sensitive washed platelets were prepared in the presence of ADP scavenger apyrase and used at 2×10^8/ml. % of platelet aggregation in response to indicated dose of ADP were analyzed. See also Figure 3Cvii. Data are represented as scatter plots with mean ± SEM from 4-8 biological replicates, one-way ANOVA with Tukey's test.

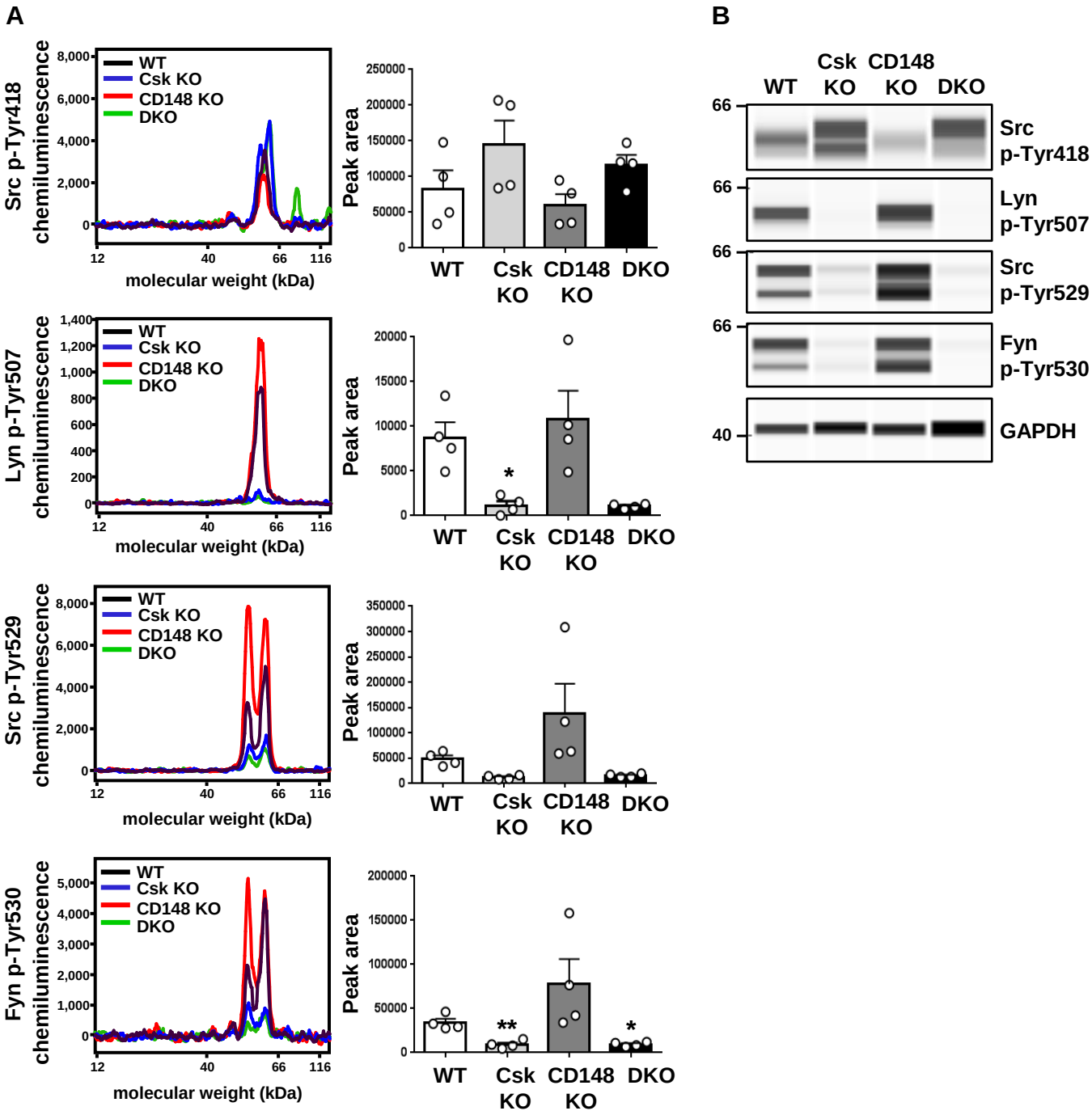

Figure S8. Increased megakaryocyte SFK activity in *Csk KO* mice. SFK activation loop and inhibitory tyrosine phosphorylation levels in bone marrow-derived megakaryocytes. (A) Representative electropherograms of capillary-based immunoassays on *ex vivo* differentiated megakaryocyte lysates with the indicated antibodies and the quantification of peak areas, n=4 mice/genotype. (B) Representative data from i) displayed as blots. *$P < 0.05$, **$P < 0.01$, RM one-way ANOVA with Tukey's test, mean ± SEM.

A Collagen stimulation

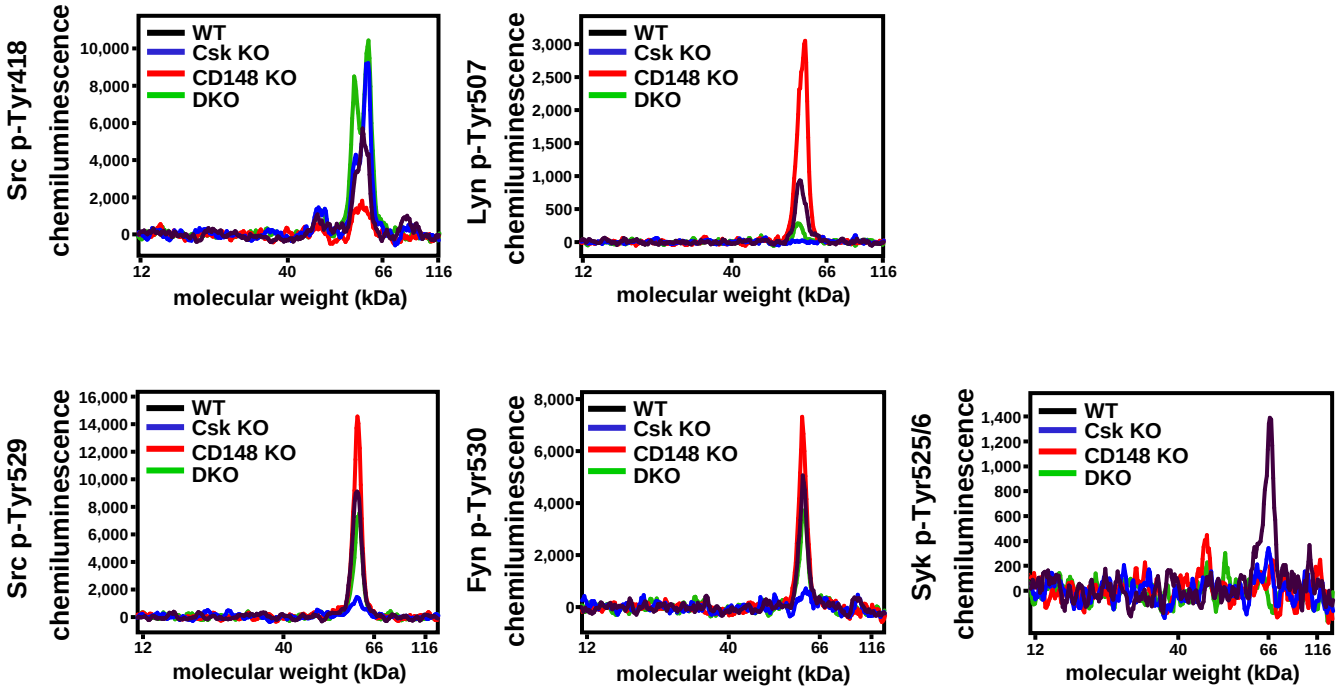

B CLEC-2 antibody stimulation

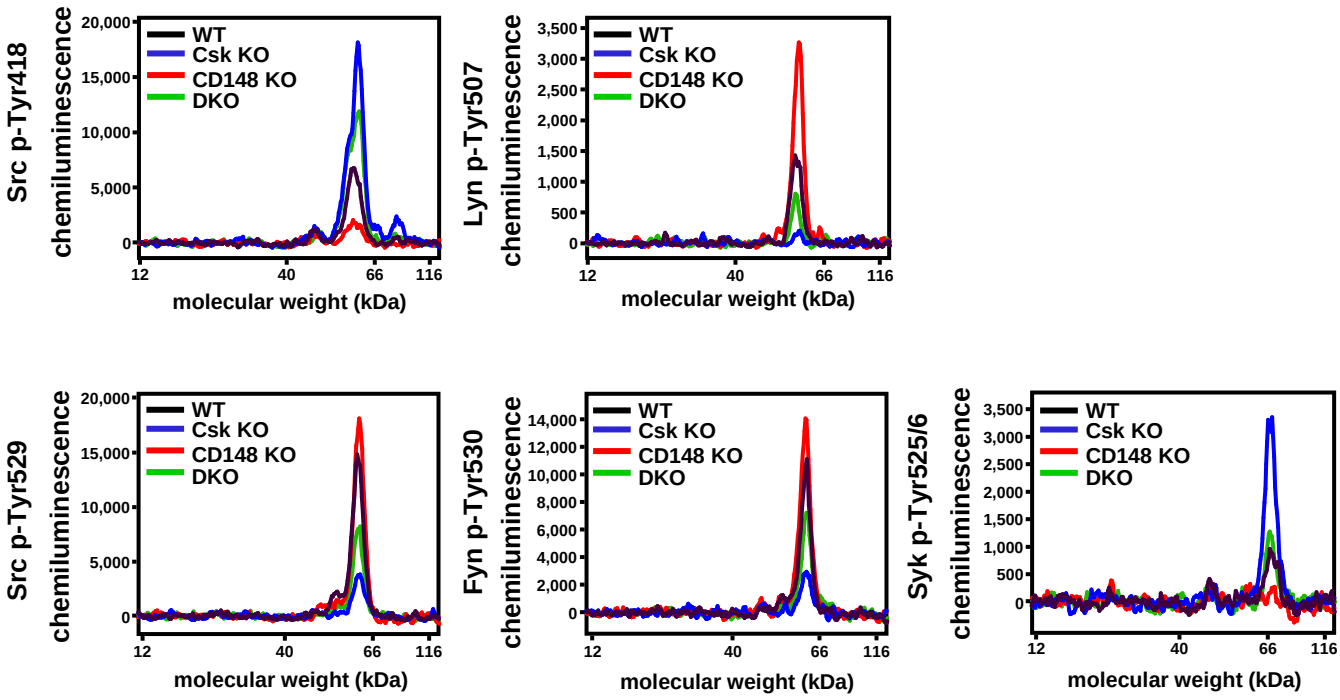

C Fibrinogen stimulation

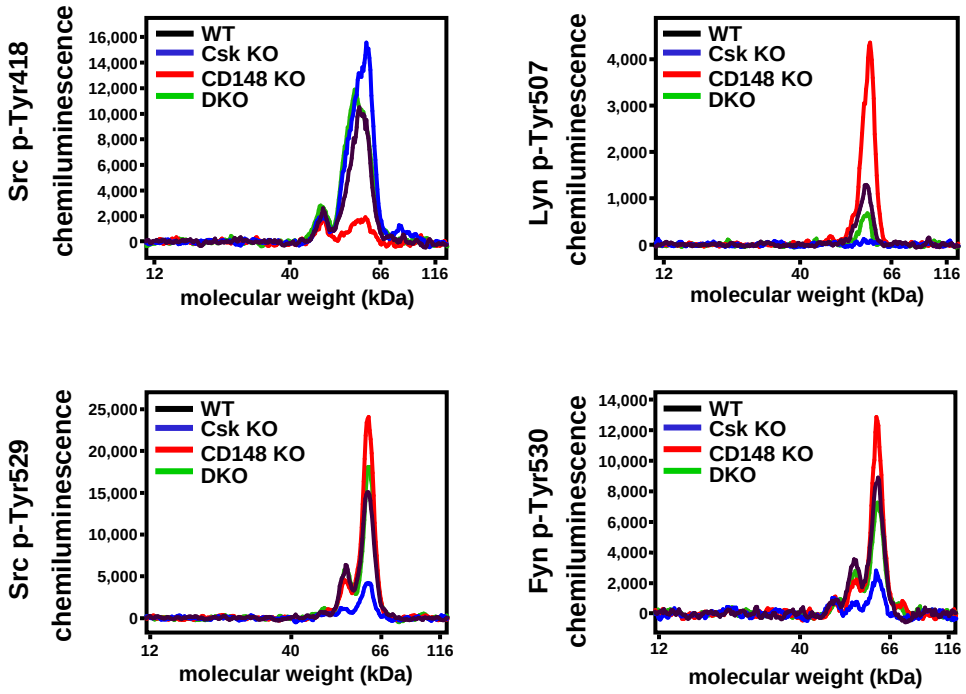

D

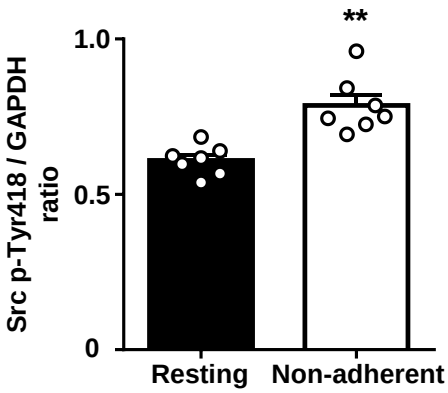

Figure S9. SFK activation loop and inhibitory tyrosine phosphorylation levels in activated platelets in *Csk KO*, *CD148 KO* and *DKO* mice. (A-C) Representative electropherograms of capillary-based immunoassays on platelet lysates with the indicated antibodies. Platelets were stimulated with A) collagen (30 μg/ml, 90 seconds), B) CLEC-2 antibody (10 μg/ml, 5 minutes) or C) were allowed to spread on fibrinogen-coated plates (100 μg/ml, 45 minutes, 37°C). (D) Src p-Tyr418 / GAPDH peak area ratio of resting and non-adherent *WT* platelets from fibrinogen-coated plates (100 μg/ml, 45 minutes, 37°C). Lysates were analyzed by capillary-based immunoassays for Src p-Tyr418 and GAPDH, n = 7 mice. **P < 0.01, paired, two-tailed t-test, mean ± SEM.

A CRP stimulation (*Csk*^{AS} platelets)

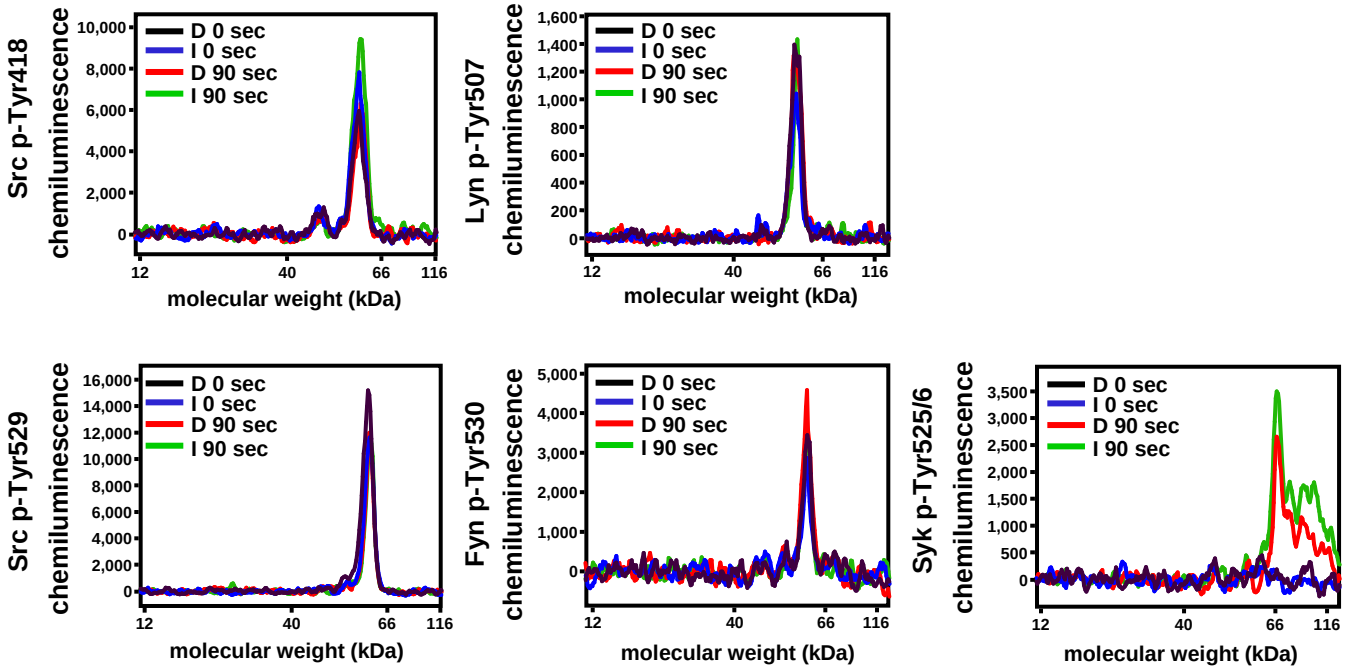

B CLEC-2 antibody stimulation (*Csk*^{AS} platelets)

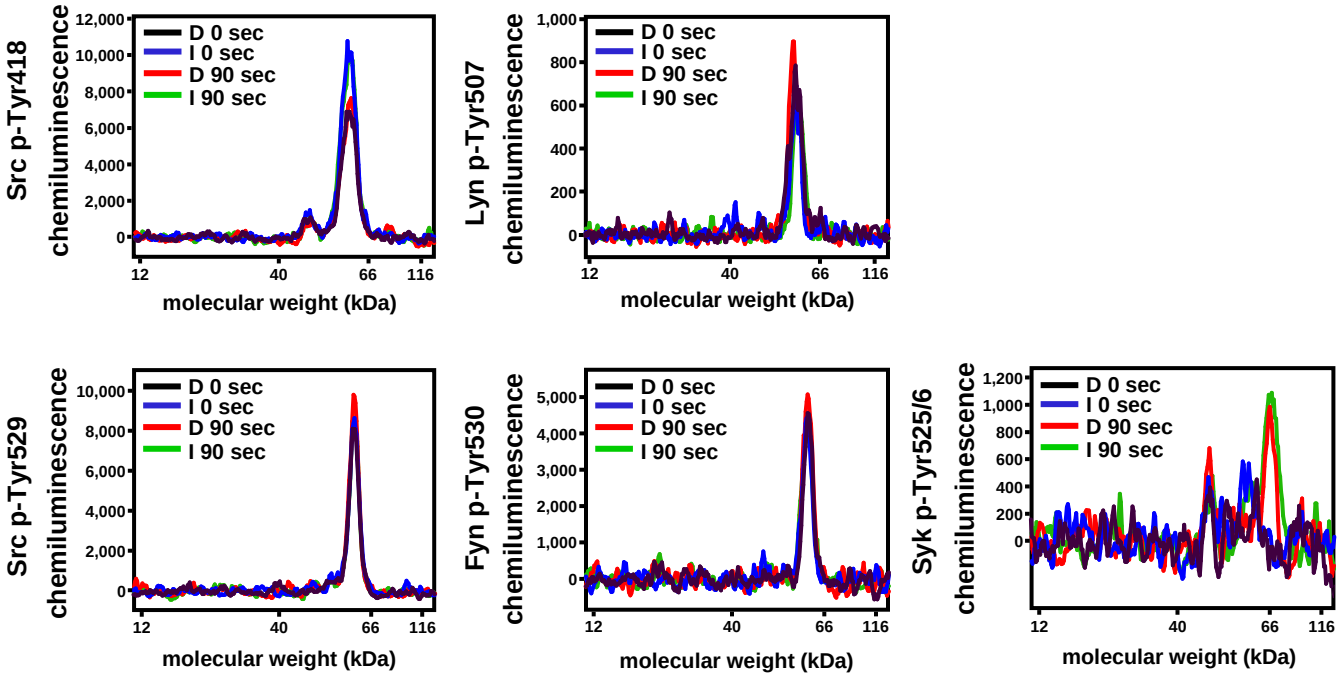

Figure S10. SFK activation loop and inhibitory tyrosine phosphorylation levels in activated platelets in *Csk*^{AS} mice. (A-B) Representative electropherograms of capillary-based immunoassays on platelet lysates with the indicated antibodies. Platelets from *Csk*^{AS} mice were pre-treated with either DMSO (D) or 10 μM 3-IB-PP1 (I) for 10 minutes and stimulated with A) CRP (30 μg/ml) or B) CLEC-2 antibody (10 μg/ml) for indicated times.

Videos

Video 1. Representative laser-induced thrombus formation in *WT, Csk KO, CD148 KO and DKO* mice.

Video 2. Representative laser-induced fibrin formation in *WT, Csk KO, CD148 KO and DKO* mice.

Video 3. Representative ferric chloride-induced thrombus formation in *WT*, *Csk KO, CD148 KO and DKO* mice.